

Physics of heavy-quark production in quantum chromodynamics

Stanley J. Brodsky

Stanford Linear Accelerator Center, Stanford, California 94305

John F. Gunion

Department of Physics, University of California, Davis, California 95616

Davison E. Soper

Institute of Theoretical Science, University of Oregon, Eugene, Oregon 97403

(Received 11 May 1987)

For very heavy quark masses, QCD predicts that the inclusive hadronic production of heavy quarks is governed by quark and gluon hard-scattering subprocesses. On general grounds, one expects corrections of order μ/M_Q , where $\mu \sim 300$ MeV and M_Q is the heavy-quark mass. At the charm mass scale, such corrections could be important, possibly accounting for the anomalies observed in the nuclear-number dependence, the longitudinal-momentum distributions, and beam-flavor dependence of charm hadroproduction. In this paper we present a general overview of such corrections. In particular, we discuss a "coalescence" correction, which substantially alters the cross section in situations where the heavy quark is known to have a low velocity relative to one or more constituents of the spectator jet. In attractive channels the result is a large enhancement. In inclusive cross sections this final-state-interaction effect is suppressed by only a single power of the heavy-quark mass.

I. INTRODUCTION

The calculation of heavy-quark production is one of the most important applications of QCD, both for predicting the production rate of new strongly interacting particles, and for assessing the backgrounds to other types of new physics. In a recent analysis, Collins, Soper, and Sterman¹ have argued that the proof of factorization for massive lepton pairs² in perturbative QCD can be generalized to the production of heavy quarks, $M_Q^2 \gg \Lambda_{\overline{\text{MS}}}^2$ ($\overline{\text{MS}}$ denotes the modified minimal-subtraction scheme). However, this argument applies only to the inclusive cross section in leading order in $1/M_Q$. It leaves open the possibilities (a) that there are large corrections to the inclusive cross section, scaling as μ/M_Q (where μ is a typical light-hadron mass of order $\Lambda_{\overline{\text{MS}}}$), and (b) that the perturbative Born term is completely unreliable for a restricted class of kinematic configurations of a semi-inclusive cross section in which another particle is detected as well as the heavy quark—only the inclusive integral over the second particle need exhibit factorization.

In fact, we can identify a specific nonperturbative effect, which we term "coalescence," that leads to effects of both types. For this purpose, it is useful to consider the semi-inclusive cross section in which the momentum of a spectator quark in the final state is measured. In this case, it has been argued³ that there are large enhancements to the cross section at low relative velocity between the spectator and the heavy quark in an attractive channel, analogous to the Schwinger correction⁴ to e^+e^- annihilation near the threshold for production

of a heavy-quark pair. In this paper, we explore QED analogues to heavy-quark production that exhibit both asymptotic factorization for the inclusive cross section and, on the other hand, large nonperturbative corrections coming from low-relative-velocity configurations.

The factorization analysis of Ref. 1 is largely limited to low-order diagrams. However, there exists in QED an all-orders (in $Z\alpha$) result, due to Bethe and Maximon,⁵ for a closely analogous heavy-particle production process—namely, the Bethe-Heitler cross section for ultrarelativistic lepton pair production in a strong Coulomb field. One may ask whether this all-orders result is consistent with factorization. In order to display the physics of this process as clearly as possible, we shall present a new derivation of the Bethe-Maximon results in Sec. II, based on high-energy eikonal analysis. The derivation explicitly demonstrates that the ultrarelativistic Bethe-Heitler cross section does, indeed, take a factorized form. This increases our confidence that the analogous factorization works in QCD to all orders in the strong coupling constant.

One may also consider the Bethe-Heitler cross section for lepton pair production in a strong Coulomb field in the case in which the negative lepton is produced with low velocity relative to the spectator nucleus. One obtains a significant enhancement in the cross section.⁶ This effect results from the attractive binding force between the negative lepton and the positively charged nucleus. In Sec. III we analyze a similar situation of direct experimental interest: production of a heavy particle in the presence of a spectator system composed of light particles. Using the Coulomb approximation, we demonstrate that QED predicts a strong enhancement in

the cross section when the heavy particle and spectator system have similar velocities and are in an attractive charge configuration. It takes the same form: namely, a Sommerfeld-type Coulomb-correction factor to the Born cross section. We also show that such enhancements are entirely consistent with factorization for the inclusive cross section, yielding possibly large order- μ/M_Q higher-twist corrections.

In the final sections we assume that analogous results will be obtained in QCD for heavy-quark production in hadronic reactions. Replacing charge by color and the electromagnetic coupling by the strong coupling, we can pursue the impact of the specific results obtained in Secs. II and III upon important phenomenological issues for charm production. We conclude with an overview of theoretical predictions for nonperturbative QCD corrections to heavy-quark production cross sections.

Before proceeding, we wish to motivate the reader by enumerating the reasons why heavy-quark hadroproduction plays a critical role in particle-physics phenomenology.

(1) For a large quark mass or large jet transverse momentum compared to the QCD scale $\Lambda_{\overline{MS}}$, the perturbative predictions are unambiguous and thus serve as important checks of QCD and the factorization theorems.^{1,2}

(2) Since the $gg \rightarrow Q\bar{Q}$ subprocess is generally dominant, heavy-quark production cross sections give essential checks on the gluon distribution of hadrons.

(3) QCD predicts a number of novel features for the hadroproduction of heavy quarks, such as forward-backward asymmetries^{7,8} in $p\bar{p}$ collisions, and exclusive channel dominance near threshold.⁹

(4) An understanding of heavy-quark production is necessary to project the rate for new-particle production—including new vector bosons, Higgs particles, supersymmetric hadrons, etc.

(5) Heavy-quark events must be understood in order to unravel single and multiple prompt lepton signals, flavor-mixing parameters, and backgrounds to rare processes.

(6) The muon content of high-energy cosmic-ray showers depends in detail on the properties of charm photoproduction and hadroproduction.¹⁰

(7) Most interesting from the theoretical point of view are the intriguing anomalies in the data for charm hadroproduction, since they are difficult to explain from standard perturbative QCD. The observed x_F charmed-hadron distributions appear flatter than predicted by primary “fusion” subprocesses.^{11–13} The dependence of the cross section on the nuclear number in fixed-target experiments is significantly less than additive.¹⁴ The cross section for the charmed-strange baryon $A^+(csu)$ produced by incident $\Sigma^-(sdd)$ beams appears anomalously large.^{15,16} Finally there are hints from the European Muon Collaboration (EMC) deeply inelastic muon-scattering experiments¹⁷ that the charmed sea distribution in the proton may be larger than predicted by standard evolution. An essential question is then whether the charm mass scale is sufficiently large such that charm hadroproduction in all kinematic domains is safe-

ly in the QCD perturbative domain, or whether the above empirical anomalies might be providing new insights into physics at the interface between perturbative and nonperturbative QCD.

Let us review the standard QCD analysis. The factorization formula

$$d\sigma = \sum_{ab} \int_0^1 dx_a \int_0^1 dx_b G_{a/A}(x_a, M_Q) \times G_{b/B}(x_b, M_Q) d\hat{\sigma}_{ab \rightarrow cd} \quad (1)$$

gives the dominant contribution to the heavy-quark production cross section to leading order in μ/M_Q . We implicitly assume that we are integrating over a range of p_T and mass of the $Q\bar{Q}$ system, and that the transverse momenta of the individual Q and \bar{Q} are not much larger than M_Q . One calculates $\hat{\sigma}$ as an expansion in $\alpha_s(M_Q^2)$. The factorization formula gives the total inclusive cross section. Thus, diffractive processes, to the extent that they contribute at leading order in μ/M_Q , are already included and should not be added separately.¹⁸

Although the physical arguments are convincing, a complete proof that factorization gives the leading power-law contribution to the cross section is highly nontrivial and has only been outlined.¹ For instance, one difficult aspect of the analysis is the subtlety concerned with initial-state elastic interactions and their possible effect on color averaging.¹⁹ An explicit demonstration that these interactions do not destroy factorization has not yet been given, except in the case where the subprocess amplitude corresponds to annihilation into a color singlet, as in massive-lepton-pair production.²

The dominant short-distance subprocesses contributing to the inclusive heavy-quark production cross section are the $gg \rightarrow Q\bar{Q}$ and $q\bar{q} \rightarrow Q\bar{Q}$ fusion reactions. The dominant contribution to the integrated cross section from these processes arises from the region $p_T \sim M_Q$. The distribution of either heavy quark is relatively flat for small rapidity, but vanishes rapidly at large Feynman x_F . However, we can also examine regions in which one of the heavy quarks is produced with $p_T \gtrsim M_Q$. In these regions two-to-three subprocesses, such as $gg \rightarrow gQ\bar{Q}$, begin to be as important as the two-to-two subprocesses. The former have been calculated in Refs. 7 and 8. [When p_T is so much greater than M_Q that $\ln(p_T/M_Q) \sim 1/\alpha_s$, a more complicated formula, involving, for instance, heavy quarks as constituents of the proton,²⁰ is necessary.]

As emphasized in Ref. 7, the region in which the final gluon has large p_T and recoils against a $Q\bar{Q}$ system with invariant mass $\sim M_Q$ is of special interest, as are the corresponding regions in $\gamma\gamma \rightarrow \gamma Q\bar{Q}$ and $\gamma\gamma \rightarrow gQ\bar{Q}$ in which the final γ and g , respectively, have large p_T . In such configurations the Q and \bar{Q} are isolated kinematically and can have small relative velocity. This is a convenient and important experimental testing ground for the nonperturbative corrections that are the focus of this paper. We shall return to discuss these processes in the conclusion.

We conclude this introduction by summarizing the important uncertainties in theoretical predictions for

heavy-quark production.

(1) Higher-order corrections in α_s . Although the two-to-three tree subprocesses have been evaluated^{7,8} the virtual one-loop corrections to the two-to-two amplitudes have not yet been calculated. In view of the large color couplings of incident gluons, one might expect a large “K” factor correction to the Born results.

(2) Order- μ/M_Q corrections. We identify four such higher-twist effects: (a) The relation between the heavy-quark mass and the measured $Q\bar{Q}$ bound-state mass is uncertain. This results in a substantial numerical uncertainty in the charm-quark production cross section; for higher-mass quarks this sensitivity is considerably less. (b) As first shown for the Drell-Yan process, one must satisfy a “target-length” condition²¹ in order that inelastic initial-state interactions do not ruin factorization: the active quark or gluon energy must be large compared to a scale proportional to the length of the target: $x_{as} > M_N L_A \mu^2$ where μ^2 is a typical hadron scale and L_A is the length of the target in its rest frame. (c) It is possible for the incoming beam particle wave function to contain “intrinsic” heavy-quark states, e.g., $|qqqQ\bar{Q}\rangle$. These have been explored in Ref. 22. The probability of such virtual states scales as $1/M_Q^2$. These virtual states live for a time of order $1/M_Q$ in their rest frame, unless a collision provides the necessary energy for their materialization. In normal collisions this energy is provided via a hard interaction and the net cross section is suppressed with respect to gluon fusion by μ^2/M_Q^2 (Ref. 23). However, if one violates the target-length condition given previously, by using a very thick nuclear target, then multiple soft collisions can accumulate to allow intrinsic heavy quarks to materialize with a cross section equal to the probability of the intrinsic state times the beam-nucleus elastic cross section.²⁴ (d) Interactions of spectator partons with the produced heavy quarks can lead to large order- μ/M_Q corrections to the totally inclusive heavy-quark cross section and to significant enhancements of semi-inclusive cross sections in particular regions of phase space—the coalescence enhancement.

Of the above effects, intrinsic heavy-quark states and the coalescence phenomena have the potential of providing a unique probe of the boundary between perturbative and nonperturbative QCD. The focus of this paper is upon the physics of coalescence and its consistency with factorization.

II. PRODUCTION OF RELATIVISTIC MUON PAIRS IN AN EXTERNAL COULOMB FIELD

In this section we will investigate the process $\gamma \rightarrow \mu^+ + \mu^-$ in the presence of the Coulomb field of a nucleus of charge Ze (treated as pointlike and infinitely massive). Our investigation extends and makes more precise the results in the Appendix of Ref. 1. We suppose that the photon energy is much larger than the muon mass M , so that the produced muons are highly relativistic. The ultrarelativistic cross section was calculated to all orders in the classic paper of Davies, Bethe, and Maximon in 1954 (Ref. 5). The process of lepton

pair production in a Coulomb field is of interest as a test of quantum electrodynamics, but our interest in it here stems from its similarity to heavy-quark production in the gluon field of a hadron. We are, therefore, interested not so much in the results as in certain key features of the physics that are important in the derivation. In particular, we are interested in the dependence of the physics on the muon mass.

In order to illustrate the physics in as simple a fashion as possible, we will replace the incident photon and the muons by scalar particles. The derivation including spin would involve a certain amount of added complexity without introducing any essential new physics.

A by-product of our investigation is a rederivation of the Davies-Bethe-Maximon results (modified for scalar particles) using modern techniques that simplify the derivation enormously.²⁵

We begin by defining the kinematics. We choose to work in the reference frame of the nucleus. We will denote four-vectors by their components $V^\mu = (V^+, V^-, \mathbf{V})$, where $V^\pm = (V^0 \pm V^3)/2^{1/2}$ and \mathbf{V} denotes the transverse components of V^μ . The kinematics of the lowest-order diagram are defined in Fig. 1. We let the momentum of the incident photon be

$$k^\mu = (P, 0, \mathbf{0}), \quad (2)$$

where P is to be very large, much larger than the muon mass M . The muon momenta are

$$l_C^\mu = (z_C P, (I_C^2 + M^2)/2z_C P, l_C), \quad (3)$$

$$l_D^\mu = (z_D P, (I_D^2 + M^2)/2z_D P, l_D),$$

where we take the momentum fractions z_C and z_D to be finite fractions of 1. The net momentum transfer q^μ from the field obeys $q^0 = 0$, so that

$$q^+ = -q^-. \quad (4)$$

From momentum conservation, we conclude that

$$q^- = (I_C^2 + M^2)/2z_C P + (I_D^2 + M^2)/2z_D P, \quad (5)$$

$$\mathbf{q} = l_C + l_D, \quad z_C + z_D = 1 + q^+ / P \approx 1.$$

We now can make an important observation. Consider the muon line carrying momentum $l_D - q$ in the lowest-order diagram, Fig. 1. We shall assume that I_C^2 and I_D^2 are not much larger than M^2 . This is indeed the case in the integration region that provides the dominant contribution to the total cross section. Then

$$(l_D - q)^+ \simeq z_D P \sim P, \quad (6)$$

$$(l_D - q)^- = -l_C^- = -(I_C^2 + M^2)/2z_C P \sim M^2/P.$$

Consequently, the space-time separation Δx^μ between the two electromagnetic vertices obeys

$$\Delta x^- \sim 1/P, \quad \Delta x^+ \sim P/M^2. \quad (7)$$

Thus both Δx^+ and Δx^- as viewed in the dimuon rest frame are of order $1/M$; Lorentz-contraction factors M/P and P/M then give the results (7) in the nucleus rest frame. Also, in order for the virtual muon to have a significant amplitude to propagate over the interval Δx^μ ,

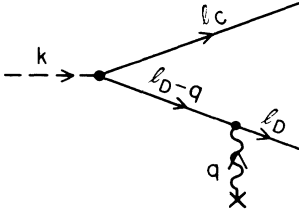


FIG. 1. Lowest-order diagram for lepton pair production on a heavy nucleus.

$(\Delta\mathbf{x})^2$ cannot be much larger than $\Delta x^+ \Delta x^-$:

$$\Delta\mathbf{x} \sim 1/M. \quad (8)$$

Thus, when the muon mass M is large, there must be short-distance scattering: the interactions that create the muon pair take place within a space-time volume in the form of a hypercube with sides of length $1/M$ as viewed in the dimuon rest frame.

In the nucleus rest frame, this volume appears stretched by a factor P/M , so that the initial creation of the virtual-muon pair occurs long before the pair reaches the region in which there is a significant field, as indicated in Fig. 2. The transverse separation r between the muons, which is boost invariant, is of order M^{-1} .

We are now in a position to estimate the cross section and to determine what values of the impact parameter \mathbf{b} give important contributions to the cross section. There are two cases. First, $|\mathbf{b}|$ can be of order $1/M$. The contribution to the cross section from this region is of order

$$\alpha(Z\alpha)^N \pi \mathbf{b}^2 \sim \alpha(Z\alpha)^N / M^2 \quad (9)$$

at order $N+1$ in α , $N=2,3,4,\dots$. Second, $|\mathbf{b}|$ can be much larger than $1/M$. In this case there is a partial cancellation because the muon pair is electrically neutral. The field interacts only with the electric dipole moment of the pair, which is of order $e|\mathbf{r}| \sim e/M$. The interaction is proportional to the transverse gradient of the potential, integrated along the path of the muon pair:

$$\int dz E_T \sim Ze \int dz |\mathbf{b}| / (z^2 + \mathbf{b}^2)^{3/2} \sim Ze / |\mathbf{b}|.$$

Thus, the contribution to the cross section from impact parameters large compared to $1/M$ is of order

$$(Z^2 \alpha^3 / M^2) \int d^2\mathbf{b} \theta(|\mathbf{b}| \gg 1/M) / |\mathbf{b}|^2 \sim (Z^2 \alpha^3 / M^2) \ln(LM). \quad (10)$$

Here we have noted that the integral is logarithmically divergent at large b and we have supposed that the Coulomb potential is cut off at distances greater than some large screening distance L (e.g., the size of the atom in which the muon pair is created). We shall dis-

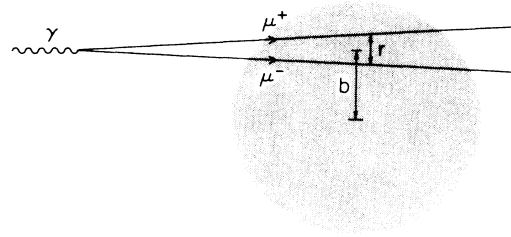


FIG. 2. Lepton pair production in the field of a nucleus, viewed from the nuclear rest frame.

cuss what happens if the infrared cutoff is removed later in this section.

Equation (10) applies at lowest order in $Z\alpha$. At order $(Z\alpha)^N$ we would have a contribution

$$\alpha(Z\alpha/M)^N \int d^2\mathbf{b} \theta(|\mathbf{b}| > b_{\min}) / |\mathbf{b}|^N \sim \alpha(Z\alpha)^N (1/M^2) (1/b_{\min} M)^{N-2},$$

where, by hypothesis, $b_{\min} M \gg 1$. Thus, the higher-order contributions in $(Z\alpha)$ to the region $|\mathbf{b}| \gg 1/M$ are suppressed by powers of M .

We may draw some conclusions from the discussion so far.

(1) The cross section is of order $1/M^2$, as expected on dimensional grounds in a theory with a dimensionless coupling.

(2) The $b \sim 1/M$ contribution is entirely controlled by short distances of order $1/M$. Thus, it involves the running coupling $\alpha(\mu)$ at a mass scale $\mu \sim M$. The cross section will obtain contributions from this short-distance region at all orders of $Z\alpha$.

(3) In the case of heavy-lepton-pair production $\gamma Z \rightarrow \tau^+ \tau^- Z$ on a realistic nucleus, the higher Born corrections ($N > 2$) will be suppressed by the factor $(R_A m_\tau)^{-(N-2)}$ since the nuclear form factor allows significant contributions only from the region $b \gtrsim R_A$.

(4) The $b \gg 1/M$ contribution is partly controlled by long distances, which in the QCD-analogue problem must be treated nonperturbatively. However, only the lowest order in $Z\alpha$ is important. We shall interpret the factor that represents the "soft" physics as the probability of finding a photon in the field of the nucleus, analogous to the probability of finding a gluon in a hadron.

We now refine our conclusions by doing a detailed calculation. Since the muons are highly relativistic, an eikonal approximation suffices to treat their interaction with the external field. There are two main ingredients. The first is the energy denominator (or, more accurately, the k^- denominator) for the virtual dimuon state before its encounter with the Coulomb field, which becomes a Bessel function after Fourier transforming with transverse momentum to transverse position:

$$\frac{1}{(2\pi)^2} \int d^2\boldsymbol{\kappa} e^{-i(\mathbf{x}_C - \mathbf{x}_D) \cdot \boldsymbol{\kappa}} \frac{1}{(\boldsymbol{\kappa}^2 + M^2)/2z_C P + (\boldsymbol{\kappa}^2 + M^2)/2z_D P} = (2z_C z_D P / 2\pi) K_0(M |\mathbf{x}_C - \mathbf{x}_D|). \quad (11)$$

The second ingredient is the eikonal phase $\chi(\mathbf{x})$ accumulated by the muon as it travels through the Coulomb field at a transverse position \mathbf{x} :

$$\chi(\mathbf{x}) = -e \int_{-\infty}^{\infty} dx^+ A^-(x^+, 0, \mathbf{x}) = -Z\alpha \ln(4z_{\max}^2 / \mathbf{x}^2), \quad (12)$$

where we have supplied a length z_{\max} as an infrared cutoff. Recall that we simplify the calculation a bit by using a spin-zero initial photon and spin-zero muons. Thus, there are no numerator factors. The coupling between the scalar photon and the scalar quarks has dimensions of mass. We take it to be Me . (In the more complicated case of spin- $\frac{1}{2}$ quarks, the factor of M arises from the numerator factor.) Following the techniques found in Refs. 26 and 1, we can write the scattering amplitude as

$$\begin{aligned} \langle C, D | S | A \rangle &= -\delta(1-z_C-z_D)2Mez_Cz_D \int d^2\mathbf{x}_C \int d^2\mathbf{x}_D \exp[-i(l_C \cdot \mathbf{x}_C + l_D \cdot \mathbf{x}_D)] \\ &\quad \times K_0(M | \mathbf{x}_C - \mathbf{x}_D |) \{ \exp[i\chi(\mathbf{x}_C) - i\chi(\mathbf{x}_D)] - 1 \} \\ &= -\delta(1-z_C-z_D)2Mez_Cz_D \int d^2\mathbf{x}_C \int d^2\mathbf{x}_D \exp[-i(l_C \cdot \mathbf{x}_C + l_D \cdot \mathbf{x}_D)] \\ &\quad \times K_0(M | \mathbf{x}_C - \mathbf{x}_D |) [(\mathbf{x}_C^2/\mathbf{x}_D^2)^{iZ\alpha} - 1] . \end{aligned} \quad (13)$$

Notice that because the muon and antimuon have opposite charges the dependence on z_{\max} cancels between the two eikonal phases.

The cross section obtained from this scattering amplitude is

$$\begin{aligned} d\sigma/dz_C dz_D &= \frac{1}{2}M^2 e^2 z_C z_D \delta(1-z_C-z_D) (2\pi)^{-3} \\ &\quad \times \int d^2\mathbf{x}_C \int d^2\mathbf{x}_D K_0(M | \mathbf{x}_C - \mathbf{x}_D |)^2 [2 - (\mathbf{x}_C^2/\mathbf{x}_D^2)^{+iZ\alpha} - (\mathbf{x}_C^2/\mathbf{x}_D^2)^{-iZ\alpha}] . \end{aligned} \quad (14)$$

The integral is easily performed. (The details are relegated to the Appendix.) The result is

$$\begin{aligned} d\sigma/dz &= (d\sigma/dz)_{\text{Born}} + (e^2/12\pi M^2)z(1-z)(Z\alpha)^2 [\psi(1-iZ\alpha) + \psi(1+iZ\alpha) + 2\gamma] \\ &= (d\sigma/dz)_{\text{Born}} + (e^2/12\pi M^2)z(1-z)2 \sum_{n=0}^{\infty} (-1)^n \zeta(2n+3) (Z\alpha)^{2n+4} , \end{aligned} \quad (15)$$

where we have used

$$z = z_C, \quad 1-z = z_D , \quad (16)$$

and where $\psi(x) = d \ln[\Gamma(x)]/dx$, $\gamma = 0.577 \dots$ is Euler's constant, and $\zeta(N)$ is the Riemann ζ function. We shall discuss the lowest-order cross section, $(d\sigma/dz)_{\text{Born}}$, below; it is infrared divergent for the unscreened Coulomb potential in the approximation used to derive Eq. (14).

Let us make three comments concerning the higher-order terms in Eq. (15). First, the result of Davies, Bethe, and Maximon, which includes spin for the incoming photon and leptons, is similar but somewhat more complicated. Second, the physics behind this result, namely, the eikonal approximation, is quite simple (although this simplicity is not evident in the Davies-Bethe-Maximon derivation). Third, as already noted by these authors, the higher-order contributions come from the short-distance region $|\mathbf{x}_C|, |\mathbf{x}_D| \sim 1/M$.

We now turn to the Born term, paying special attention to the infrared behavior. We may write the Born term as

$$\begin{aligned} (d\sigma/dz)_{\text{Born}} &= (M^2 e^2/4\pi)(Ze^2)^2 z(1-z)\mu^\epsilon \int \frac{d^{2-\epsilon}\Delta}{(2\pi)^{2-\epsilon}} \mu^\epsilon \int \frac{d^{2-\epsilon}\mathbf{q}}{(2\pi)^{2-\epsilon}} \frac{1}{[\mathbf{q}^2 + q_z^2 + (1/L)^2]} \\ &\quad \times \left[\frac{1}{\{[(1-z)\mathbf{q} - \Delta]^2 + M^2\}^2} + \frac{1}{[(z\mathbf{q} + \Delta)^2 + M^2]^2} \right. \\ &\quad \left. - 2 \frac{1}{(z\mathbf{q} + \Delta)^2 + M^2} \frac{1}{[(1-z)\mathbf{q} - \Delta]^2 + M^2} \right] . \end{aligned} \quad (17)$$

We have written the result in terms of the transverse momentum \mathbf{q} of the exchanged photon and a relative transverse momentum Δ :

$$\mathbf{q} = l_C + l_D, \quad \Delta = (1-z)l_C - z l_D, \quad l_C = z\mathbf{q} + \Delta, \quad l_D = (1-z)\mathbf{q} - \Delta . \quad (18)$$

The four terms correspond to the four diagrams shown in Fig. 3. The formula has been written in $2-\epsilon$ transverse dimensions (with a dimensional regularization scale μ) for our later convenience. Equation (17) is the Born term obtained from Eq. (14), except for two modifications that affect the infrared behavior. First, we have supplied a mass $1/L$ for the exchanged photon, which means that the Coulomb field will be screened with a screening length L : $A^0 \sim (1/r)\exp(-r/L)$. Second, we have inserted the z component q_z of the photon momentum in the photon propagators. Using Eqs. (4) and (5) we have

$$q_z^2 = (q^z - q^0)^2 = (-2^{1/2}q^-)^2 = 2[(l_C^2 + M^2)/2zP + (l_D^2 + M^2)/2(1-z)P]^2 = [\Delta^2 + M^2 + z(1-z)\mathbf{q}^2]^2/2z^2(1-z)^2P^2 . \quad (19)$$

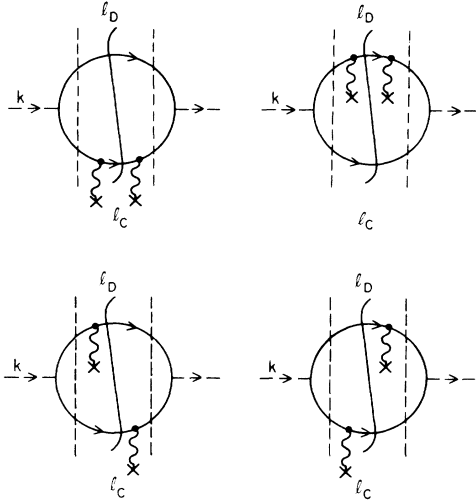


FIG. 3. Four diagrams contributing to Eq. (A17).

Since q_z^2 is proportional to $1/P^2$, it is ordinarily negligible. However, it is the only infrared cutoff in Eq. (17) in the case of an unscreened Coulomb field. The cutoff arises because, as the muon pair travels through the Coulomb field, there is a slowly varying phase factor $\exp(iq^-x^+)$ in its wave function. Thus, the line integral

$$\chi(\mathbf{x}) = -e \int_{-\infty}^{\infty} dx^+ A^-(x^+, 0, \mathbf{x})$$

should really have been (for the Born term)

$$\chi(\mathbf{x}) = -e \int_{-\infty}^{\infty} dx^+ e^{iq^-x^+} A^-(x^+, 0, \mathbf{x})$$

in lowest-order perturbation theory. This kinetic phase

factor cuts off the contribution from large x^+ , and thus eventually cuts off the contribution from large impact parameters.

We shall now write the Born term in the factorized form similar to that which would be used to calculate the cross section for heavy-particle production in high-energy hadron collisions, see Ref. 1. One must separate the part of the process that contains soft momentum transfers (and is thus not perturbatively calculable in the analogous QCD problem) from the perturbatively calculable hard-scattering factor, which contains only momenta that are of order of the heavy-particle mass M . First, we divide the Born cross section into two pieces: an infrared-sensitive piece and an ultraviolet-sensitive remainder. The ultraviolet-sensitive remainder corresponds to *photon + nucleus* \rightarrow *muon pair + nucleus* hard scattering. Second, we write the infrared-sensitive piece in a factorized form: a factor representing the distribution of photons in the Coulomb field convoluted with a hard-scattering factor for the process *photon + photon* \rightarrow *muon pair*.

We begin with the separation of the Born cross section into an infrared-sensitive piece and an ultraviolet-sensitive remainder. We define the infrared-sensitive piece as follows. We make the approximation $q^2 \ll \Delta^2, M^2$ under the integral signs and replace the resulting factor of $(2\mathbf{q} \cdot \Delta)^2$ by $[4/(2-\epsilon)]q^2\Delta^2$. (Here we use the fact that $\Delta^i \Delta^j$ multiplies a rotationally invariant integral which must be proportional to δ^{ij} .) The resulting \mathbf{q} integral is divergent at large $|\mathbf{q}|$ when $\epsilon=0$, so we subtract the ultraviolet (UV) pole. With the normal choice of μ , $\mu \sim M$, this is essentially equivalent to cutting off the \mathbf{q} integral at $q^2 \sim M^2$. This gives us the definition

$$\begin{aligned} (d\sigma/dz)_{\text{IR}} &= \frac{1}{4} M^2 e^4 z(1-z) \left[\frac{4}{2-\epsilon} \right] \mu^\epsilon \\ &\times \int \frac{d^{2-\epsilon}\Delta}{(2\pi)^{2-\epsilon}} \frac{\Delta^2}{(\Delta^2 + M^2)^4} \\ &\times \left[\frac{(Ze)^2}{\pi} \mu^\epsilon \int \frac{d^{2-\epsilon}\mathbf{q}}{(2\pi)^{2-\epsilon}} \frac{q^2}{[q^2 + (\Delta^2 + M^2)^2/2z^2(1-z)^2P^2 + (1/L)^2]^2} - (1/\epsilon)[(Ze)^2/2\pi^2] \right]. \end{aligned} \quad (20)$$

The ultraviolet-sensitive term is constructed from the remainder $(d\sigma/dz)_{\text{Born}} - (d\sigma/dz)_{\text{IR}}$. When we take this difference under the integral signs, we see that the integration region $q^2 \ll M^2$ is now *not* important. Therefore, we may neglect the infrared cutoffs q_z^2 and $(1/L)^2$. (The error thus introduced is smaller than the term retained by a power of $1/LM$ or M/P .)

The calculation of $(d\sigma/dz)_{\text{UV}}$ can be simplified as follows. As we have defined it, $(d\sigma/dz)_{\text{UV}}$ consists of two pieces. First, there is the original Born term (17) with the infrared cutoffs q_z and $1/L$ set equal to zero. When this term is evaluated using the dimensional regulation of Eq. (17), it consists of a finite piece plus a $1/\epsilon$ pole term arising from the infrared divergence that was created when the physical infrared cutoffs were eliminated. Second, there is $(d\sigma/dz)_{\text{IR}}$, Eq. (20), with the infrared cutoffs q_z and $1/L$ [as given in (19)] set equal to zero. Consider the quantity in large parentheses after the integral in Eq. (20). The \mathbf{q} integral with the infrared cutoffs removed is simply $\int d^{2-\epsilon}\mathbf{q}(1/q)^2$. This integral consist of a $1/\epsilon$ pole arising from its ultraviolet divergence plus an equal and opposite $1/\epsilon$ pole arising from its infrared divergence. The net integral is zero. Thus, the factor in the large parentheses is simply $-(1/\epsilon)(Ze)^2/2\pi^2$. We thus obtain for $(d\sigma/dz)_{\text{UV}}$ the expression

$$\left. \frac{d\sigma}{dz} \right|_{\text{UV}} = \frac{1}{4\pi} M^2 e^2 (Ze^2)^2 z(1-z) \mu^\epsilon \int \frac{d^{2-\epsilon} \Delta}{(2\pi)^{2-\epsilon}} \left[\mu^\epsilon \int \frac{d^{2-\epsilon} \mathbf{q}}{(2\pi)^{2-\epsilon}} \frac{1}{(\mathbf{q}^2)^2} \left[\frac{1}{(z\mathbf{q} + \Delta)^2 + M^2} - \frac{1}{[(1-z)\mathbf{q} - \Delta]^2 + M^2} \right]^2 + \frac{1}{\epsilon} \frac{1}{\pi(1-\epsilon/2)} \frac{\Delta^2}{(\Delta^2 + M^2)^4} \right]. \quad (21)$$

The $1/\epsilon$ term, which originated as the counterterm for the ultraviolet divergence in $(d\sigma/dz)_{\text{IR}}$, now cancels the infrared divergence in $(d\sigma/dz)_{\text{UV}}$.

The integral has the form

$$(d\sigma/dz)_{\text{UV}} = (e^2/M^2)(Ze^2)^2 z(1-z) [A \ln(\mu_{\overline{\text{MS}}}^2/M^2) + B], \quad (22)$$

where $\mu_{\overline{\text{MS}}}^2 \equiv 4\pi\mu^2 e^{-\gamma}$. This UV contribution corresponds to a hard scattering of $\gamma + \text{nucleus} \rightarrow \mu^+ \mu^- + \text{nucleus}$.

We can now study the infrared sensitive term, Eq. (20). A change of variables will make it apparent that this term has the proper factorized form. In the center-of-mass frame of the muon pair, the Coulomb field would look like a beam of photons. We define a variable x_B that represents the momentum fraction carried by the photon that is absorbed by the muons:

$$x_B = |q_z| / M_B = (\Delta^2 + M^2) / [2^{1/2} z(1-z) P M_B]. \quad (23)$$

Here M_B is introduced in order to make x_B dimensionless. It plays the role of the mass of the nucleus that produces the Coulomb field. The final result does not, of course, depend on M_B . Evidently the smallest value that x_B can assume is

$$x_{\text{min}} = M^2 / [2^{1/2} z(1-z) P M_B]. \quad (24)$$

Using x_B as the integration variable in place of Δ^2 , we find that the infrared contribution to the cross section assumes the factorized form

$$(d\sigma/dz)_{\text{IR}} = \int_{x_{\text{min}}}^{\infty} dx_B f_{\gamma/B}(x_B) d\hat{\sigma}/dz. \quad (25)$$

We now discuss the factors in this expression.

The hard-scattering cross section $d\hat{\sigma}/dz$ is

$$d\hat{\sigma}/dz = \frac{e^4 z(1-z)}{8\pi M^2} \frac{x_B/x_{\text{min}} - 1}{(x_B/x_{\text{min}})^3}. \quad (26)$$

The reader may check that this is precisely the lowest-order cross section for (scalar) photon + photon \rightarrow (scalar) μ^+ + (scalar) μ^- .

The function $f_{\gamma/B}(x_B)$ is

$$\begin{aligned} f_{\gamma/B}(x_B) &= \frac{1}{x_B} \frac{(Ze)^2}{\pi} \mu^\epsilon \int \frac{d^{2-\epsilon} \mathbf{q}}{(2\pi)^{2-\epsilon}} \frac{\mathbf{q}^2}{[\mathbf{q}^2 + x_B^2 M_B^2 + (1/L)^2]^2} - (1/\epsilon) [(Ze)^2 / 2\pi^2 x_B] \\ &= (1/x_B) (Ze/2\pi)^2 \ln\{\mu_{\overline{\text{MS}}}^2 / [x_B^2 M_B^2 + (1/L)^2]\} - 1. \end{aligned} \quad (27)$$

This function represents the distribution of photons in the Coulomb field. The first expression in Eq. (27) for $f_{\gamma/B}(x_B)$ may be independently derived by starting from the general definition²⁷

$$f_{\gamma/B}(x_B) = (2^{1/2} / 2\pi x_B M_B) \int dy^+ \exp(-iq^- y^+) \langle B | F(y^+, 0, 0)^- \cdot F(0)^{v-} | B \rangle, \quad (28)$$

where $|B\rangle$ is the state of nucleus B at rest, $q^- = x_B M_B / 2^{1/2}$, and $F^{\mu\nu}$ is the electromagnetic field-strength operator. Write the momentum eigenstates in terms of position eigenstates $|R\rangle$ [normalized to $\langle R | R' \rangle = \delta^3(R - R')$]:

$$|B\rangle = (2M_B)^{1/2} \int d^3R |R\rangle.$$

Then, using

$$F^{\mu\nu}(x)_{\text{operator}} |R\rangle = F^{\mu\nu}(x - R)_{\text{classical}} |R\rangle$$

with a screened Coulomb field for $F^{\mu\nu}(x - R)_{\text{classical}}$, the result (27) follows. One should note two features. First, the definition of Ref. 27 [cf. Eq. (28)] requires that the operator product be renormalized by minimal subtraction. Thus, the $\epsilon=0$ pole in Eq. (27) is to be subtracted. Second, in the external field approximation used here, the nucleus can absorb any amount of momentum without recoiling. Thus, momentum conservation is lost and x_B is not necessarily smaller than 1.

The integral in (25) can be performed analytically. The result when the screening cutoff $1/L$ is removed is quite simple:

$$\frac{d\sigma_{\text{IR}}}{dz} = \frac{e^2(Ze^2)^2 z(1-z)}{96\pi M^2} \left[\ln \left[\frac{(8\pi)^{1/2} z(1-z)\mu P}{M^2} \right] - \frac{5}{6} \right] \quad (1/L=0). \quad (29)$$

The value of the renormalization scale μ here is arbitrary, since the μ dependence cancels between $d\sigma_{\text{IR}}/dz$ and $d\sigma_{\text{UV}}/dz$ as given in Eq. (22). A sensible choice is $\mu \sim M$, so that $d\sigma_{\text{UV}}/dz$ is not large.

Notice the appearance of a logarithm of the initial photon energy, $P/2^{1/2}$, in the cross-section result (29). This logarithm arises from the $\ln(x_B)$ in the photon distribution function. The $\ln(x_B)$ arises, in turn, from the small- q behavior of the integrand for the photon distribution function. It reflects the probability to find a photon at a large transverse separation, $|\mathbf{b}| \sim 1/x_B M_B$, from the nucleus. If the field is screened, then there is no $\ln(P)$ in the cross section.

III. MODEL FOR COALESCENCE ENHANCEMENT

In this section we shall consider a simple model for heavy-quark production in which the effects of coalescence of the produced and spectator systems can be studied. Specifically, we examine a process as illustrated in Fig. 4, in which a heavy quark of mass M is produced and then interacts with a light spectator quark of mass m . We first examine the semi-inclusive cross section in which the spectator is detected in the final state. We find that the cross section is enhanced when the velocity of the light quark nearly matches that of the heavy quark. Next, we examine the inclusive cross section, in which the spectator quark is not observed and, in addition, the transverse momentum of the heavy quark is not observed. The factorization theorem guarantees that the effect on this inclusive cross section of such an interaction with a spectator is suppressed in the limit of large M . This suppression results from a cancellation, due to

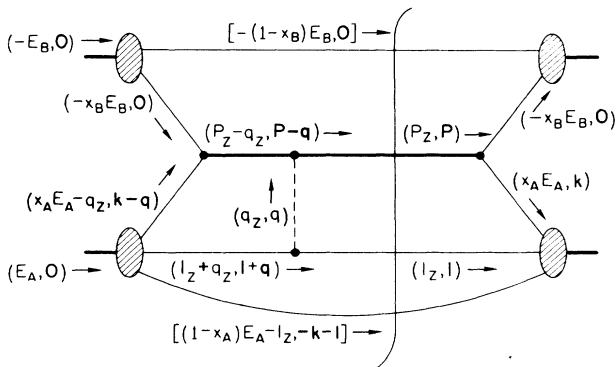


FIG. 4. Basic diagram illustrating the production of a single heavy quark Q in a hadron collision, via the subprocesses $q q \rightarrow Q$. Various spectators are shown.

unitarity, between different kinematical regions of the semi-inclusive cross section. We will see how this (partial) cancellation works in detail in the model, and evaluate the remaining correction to the perturbative factorized prediction for the cross section.

In the model, all quarks are scalars. The light quarks have mass m and the heavy quark has mass $M \gg m$. The Born subprocess is $q + q \rightarrow Q$. (It is for reasons of simplicity that we choose a model in which a *single* heavy quark can be produced from light quarks. An analogue of practical interest is gluino + quark \rightarrow squark in a model of supersymmetry in which the gluino is light and the squark is heavy.) We choose to describe the process in a reference frame in which the heavy quark is nearly at rest. In this frame, we take hadron A to contain a high-momentum quark that is active in the Born subprocess, a high-momentum spectator quark, and a spectator quark that carries low momentum. These constituents of hadron A all carry transverse momentum of order m . We suppose that hadron B contains a high-momentum quark that is active in the Born subprocess and a high-momentum spectator quark. For simplicity, we suppose that the hadron B constituents carry negligible transverse momentum.

We now add an interaction between the slow spectator quark and the heavy quark. In order to mimic QCD, we work in an Abelian gauge theory in which the heavy quark has charge e and the light quark has charge $-e$. We choose to work in Coulomb gauge. Then the leading interaction between two slow particles is the Coulomb interaction. Thus, we take the spectator-heavy-quark interaction to be a Coulomb exchange. The resulting model is depicted in Fig. 4. Of course, one has to add the graph shown and its complex conjugate. A convenient choice of kinematic variables is shown in the figure. The three-momentum of each particle is indicated in a notation in which the z component is given first, followed by a transverse vector standing for the transverse components. (We indicate three-vectors with an arrow, \vec{q} , and, as in Sec. II, transverse vectors are in bold type, \mathbf{q} , while energy and z components are explicitly indicated, or reexpressed in terms of q^+ and q^- .)

We take hadron A to have a large momentum E_A along the positive z axis, while hadron B has a large momentum E_B along the negative z axis. (We take the incoming hadrons to have zero mass for simplicity.)

We shall write the amplitude for this model using time-ordered perturbation theory. We need several ingredients. The first is the heavy-quark production vertex, which we take to be $-iG$. The second ingredient is the Coulomb potential, $+ie^2/\vec{q}^2$. The third ingredient is wave functions for the incoming hadrons. For hadron B , we use a wave function $\Psi_B(x_B)$ such that $|\Psi_B(x_B)|^2 dx_B$ is the probability to find the active

quark with momentum fraction x_B . For hadron A , we use a wave function $\Psi_A(x_A, \mathbf{k}; \vec{l})$ such that $|\Psi_A(x_A, \mathbf{k}; \vec{l})|^2 dx_A d\mathbf{k} d\vec{l}$ is the probability of finding the active quark with momentum fraction x_A and transverse momentum \mathbf{k} and the slow spectator quark with momentum \vec{l} . (For this section we adopt a notation such that $d\mathbf{k}$ is a two-dimensional transverse integration, while $d\vec{l}$ is a three-dimensional integration.) Since the bound states are stable, the wave functions may be taken

to be real valued. The final ingredients that we need are the energies of the initial state, the intermediate state between the time the heavy quark was created and the time of the Coulomb interaction, and the final states. (We do not need the energies for the states before the heavy quark was formed because the corresponding energy denominators will be included in the bound-state wave functions.) Referring to Fig. 4, we find

$$E_I = E_A + E_B, \quad (30)$$

$$E_1 = (1-x_A)E_A - l_z + \frac{(\mathbf{k}+I)^2 + m^2}{2(1-x)E_A} + (1-x_B)E_B + \frac{m^2}{2(1-x_B)E_B} + m + \frac{(\vec{l}+\vec{q})^2}{2m} + M + \frac{(\vec{P}-\vec{q})^2}{2M},$$

$$E_2 = (1-x_A)E_A - l_z + \frac{(\mathbf{k}+I)^2 + m^2}{2(1-x)E_A} + (1-x_B)E_B + \frac{m^2}{2(1-x_B)E_B} + m + \frac{\vec{l}^2}{2m} + M + \frac{\vec{P}^2}{2M}.$$

In writing these expressions, we have used the nonrelativistic approximation for the slow particles and the extreme-relativistic approximation for the fast particles.

We can now assemble these ingredients to form the cross section in which the slow spectator quark is detected. For the Born term we have

$$\left. \frac{d\sigma}{d\vec{P} d\vec{l}} \right|_{\text{Born}} = \int dx_B \Psi_B(x_B)^2 \int dx_A d\mathbf{k} \Psi_A(x_A, \mathbf{k}; \vec{l})^2 \frac{G^2}{4M^3} \delta(x_A E_A - x_B E_B - P_z) \delta^2(\mathbf{k} - \mathbf{P}) (2\pi) \delta(E_I - E_2). \quad (31)$$

For the first-order terms depicted in Fig. 4, we have

$$\left. \frac{d\sigma}{d\vec{P} d\vec{l}} \right|_{\text{1st order}} = \int \frac{d\vec{q}}{(2\pi)^3} \int dx_B \Psi_B(x_B)^2 \int dx_A d\mathbf{k} \Psi_A(x_A, \mathbf{k}; \vec{l}) \Psi_A(x_A - q_z/E_A, \mathbf{k} - \mathbf{q}; \vec{l} + \vec{q})$$

$$\times \frac{G^2}{4M^3} \delta(x_A E_A - x_B E_B - P_z) \delta^2(\mathbf{k} - \mathbf{P})$$

$$\times \frac{i}{E_I - E_1 + i\epsilon} \frac{ie^2}{\vec{q}^2} (2\pi) \delta(E_I - E_2) + \text{complex conjugate}. \quad (32)$$

These expressions can be simplified by using the δ functions to eliminate the \mathbf{k} , x_A , and x_B integrations, with

$$\mathbf{k} = \mathbf{P} \quad (33)$$

and

$$x_A = \frac{M}{2E_A} + \frac{-l_z + P_z + m}{2E_A}, \quad x_B = \frac{M}{2E_B} + \frac{-l_z - P_z + m}{2E_B}. \quad (34)$$

Here the first terms are the most important, but the small correction provided by the second terms will be needed for our calculation of the inclusive cross section because of a cancellation of the leading term in that cross section. Corrections of order $\vec{l}^2/2m$ and $\vec{P}^2/2M$ have been neglected relative to P_z and l_z in the second terms of (34), in accordance with the nonrelativistic approximation of our calculation. Terms with more powers of E_A or E_B in the denominator have been neglected.

In the first-order term, we use the energy-conserving δ function to make the replacement $E_I \rightarrow E_2$ in the energy denominator. Then Eq. (30) gives

$$E_2 - E_1 = \frac{\vec{l}^2 - (\vec{l} + \vec{q})^2}{2m} + \frac{\vec{P}^2 - (\vec{P} - \vec{q})^2}{2M} = -\vec{V} \cdot \vec{q} - \frac{\vec{q}^2}{2m_R}, \quad (35)$$

where \vec{V} is the relative velocity between the light and heavy quarks and m_R is the reduced mass of the heavy-quark-light-quark system:

$$\vec{V} = \frac{\vec{l}}{m} - \frac{\vec{P}}{M}, \quad m_R = \frac{mM}{M+m}. \quad (36)$$

Having made these manipulations in Eqs. (31) and (32), we obtain

$$\left. \frac{d\sigma}{d\vec{P} d\vec{l}} \right|_{\text{Born}} = \frac{\pi G^2}{M^3 s} \Psi_B(x_B)^2 \Psi_A(x_A, \mathbf{P}; \vec{l})^2 \quad (37)$$

and

$$\left[\frac{d\sigma}{d\vec{P}d\vec{l}} \right]_{\text{1st order}} = \frac{\pi G^2}{M^3 S} \Psi_B(x_B)^2 \int \frac{d\vec{q}}{(2\pi)^3} \Psi_A(x_A; \mathbf{P}; \vec{l}) \Psi_A(x_A - q_z/E_A, \mathbf{P} - \mathbf{q}; \vec{l} + \vec{q}) \left[\frac{2}{\vec{V} \cdot \vec{q} + \vec{q}^2/2m_R} \right]_P \frac{e^2}{\vec{q}^2}. \quad (38)$$

In writing Eq. (38), we have noted that we must take the expression computed from Eq. (32) and add its complex conjugate. The result is to change $1/(\vec{V} \cdot \vec{q} + \vec{q}^2/2m_R + i\epsilon)$ to $2/(\vec{V} \cdot \vec{q} + \vec{q}^2/2m_R)_P$, where the P indicates a principal-value prescription for the singularity.

A. Small-relative-velocity approximation

It is evident from Eq. (38) that the first-order correction to the cross section is large when the relative velocity \vec{V} is small. Let us therefore examine this correction in the limit $\vec{V} \ll 1$. We notice that the typical value of \vec{q} that contributes to the integral (38) is of order $|\vec{q}| \sim m |\vec{V}|$. Thus, when \vec{V} is very small we can set $\vec{q} = 0$ inside the second factor of Ψ_A in Eq. (38). This approximation gives

$$\left[\frac{d\sigma}{d\vec{P}d\vec{l}} \right]_{\text{1st order}} = \left[\frac{d\sigma}{d\vec{P}d\vec{l}} \right]_{\text{Born}} I(V), \quad (39)$$

where

$$I(V) = \int \frac{d\vec{q}}{(2\pi)^3} \left[\frac{2}{\vec{V} \cdot \vec{q} + \vec{q}^2/2m_R} \right]_P \frac{e^2}{\vec{q}^2}. \quad (40)$$

A straightforward calculation gives

$$I(V) = \frac{\pi\alpha}{V}. \quad (41)$$

Thus,

$$\left[\frac{d\sigma}{d\vec{P}d\vec{l}} \right] = \left[\frac{d\sigma}{d\vec{P}d\vec{l}} \right]_{\text{Born}} \left[1 + \frac{\pi\alpha}{V} \right] \quad (42)$$

in the small- V approximation. We recognize this as the familiar first-order correction to production of slow charged particles in a Coulomb field.⁶ At higher orders it becomes^{6,28}

$$\left[\frac{d\sigma}{d\vec{P}d\vec{l}} \right] = \left[\frac{d\sigma}{d\vec{P}d\vec{l}} \right]_{\text{Born}} \frac{2\pi\alpha/V}{1 - \exp(-2\pi\alpha/V)}. \quad (43)$$

We learn from this example that the coalescence enhancement is large and that it does *not* cancel when one requires that a spectator quark be detected with velocity close to that of the heavy quark. In the QCD analogue of this model, the factor α is to be replaced by α_s , times a factor that depends on the color state of the two quarks. For instance, if the heavy quark carries a $\bar{3}$ representation of color while the spectator carries a $\bar{3}$ representation and if the two quarks form a color singlet, then the factor α becomes $\frac{4}{3}\alpha_s$. The typical momentum transfer in the coalescence interaction is mV , so the argument of α_s should be roughly mV , with $m \sim 300$ MeV. Of course, the use of perturbation theory is not

strictly justified for such a small momentum transfer, so we only expect Eqs. (42) and (43) to be qualitatively correct when applied to QCD.

B. Inclusive cross section

Let us now return to Eqs. (37) and (38) for the first-order correction to the cross section and integrate over the momentum of the slow spectator quark and over the transverse momentum of the heavy quark. It will prove convenient to describe the longitudinal momentum of the heavy quark by its rapidity Y and the longitudinal momentum of the light quark by its rapidity y . Since we are assuming a nonrelativistic approximation for the heavy quark and spectator quarks, these rapidities are given by

$$Y \approx P_z/M, \quad y \approx l_z/M. \quad (44)$$

For the Born term, we obtain

$$\left[\frac{d\sigma}{dY} \right]_{\text{Born}} = \frac{\pi G^2}{M^2 S} \int d\mathbf{P} dl m dy \Psi_B(x_B)^2 \times \Psi_A(x_A, \mathbf{P}, my, l)^2, \quad (45)$$

where

$$x_A = \frac{M}{2E_A} \left[1 + Y + \frac{m}{M}(1-y) \right], \quad (46)$$

$$x_B = \frac{M}{2E_B} \left[1 - Y + \frac{m}{M}(1-y) \right].$$

If we neglect the m/M terms in x_A and x_B , then we obtain the standard factorized form:

$$\left[\frac{d\sigma}{dY} \right]_{\text{Born}} = \frac{\pi G^2}{M^2 S} f_A(\bar{x}_A) f_B(\bar{x}_B), \quad (47)$$

where

$$f_A(\bar{x}_A) = \int d\mathbf{P} dl m dy \Psi_A(\bar{x}_A, \mathbf{P}; my, l)^2, \quad (48)$$

$$f_B(\bar{x}_B) = \Psi_B(\bar{x}_B)^2,$$

and

$$\bar{x}_A = x_A^0(1+Y), \quad \bar{x}_B = x_B^0(1-Y), \quad (49)$$

with

$$x_A^0 = M/2E_A, \quad x_B^0 = M/2E_B. \quad (50)$$

For the first-order term, we obtain, in terms of x_A and x_B defined in Eq. (46),

$$\left. \frac{d\sigma}{dY} \right|_{\text{1st order}} = \frac{\pi G^2}{M^2 S} \int d\mathbf{P} dl m dy \frac{d\vec{q}}{(2\pi)^3} \Psi_B(x_B)^2 \Psi_A(x_A, \mathbf{P}; my, l) \\ \times \Psi_A \left[x_A + x_A^0 \frac{m}{M} \left[-2 \frac{q_z}{m} \right], \mathbf{P} - \mathbf{q}; my + q_z, l + \mathbf{q} \right] \frac{2}{[(y - Y)q_z + \mathbf{V} \cdot \mathbf{q} + \vec{q}^2 / 2m_R]_P} \frac{e^2}{\vec{q}^2}. \quad (51)$$

We know on general grounds (see Ref. 1) that the large enhancement for small relative velocities that we noted in the previous subsection must cancel when we integrate over velocities and thus form the inclusive cross section. The enhancement arises because the intermediate-state energy denominator becomes small when V is small. That is, there is an enhancement because the attractive quark-quark interaction has a long time to occur when V is small. However, because time evolution is governed by a unitary matrix, interactions that occur long after the heavy quark has been produced do not affect the probability for the hard interaction that produced the heavy quark.

We will not rely on the general argument here, but will explicitly display the cancellation that eliminates the leading term in the enhancement. To do so, let us make a change of integration variables:

$$y' = y + q_z / m_R, \quad q'_z = -q_z, \\ \mathbf{P}' = \mathbf{P} - \mathbf{q}, \quad l' = l + \mathbf{q}, \quad \mathbf{q}' = -\mathbf{q}. \quad (52)$$

$$\left. \frac{d\sigma}{dY} \right|_{\text{1st order}} = \frac{\pi G^2}{M^2 S} \int d\mathbf{P} dl m dy \frac{d\vec{q}}{(2\pi)^3} \Psi_B \left[x_B - x_B^0 \frac{m}{M} \frac{q_z}{m_R} \right]^2 \\ \times \Psi_A \left[x_A + x_A^0 \frac{m}{M} \left[\frac{2q_z}{m} - \frac{q_z}{m_R} \right], \mathbf{P}; my + \frac{m}{M} q_z, l \right] \\ \times \Psi_A \left[x_A + x_A^0 \frac{m}{M} \left[-2 \frac{q_z}{m} + 2 \frac{q_z}{m} - \frac{q_z}{m_R} \right], \mathbf{P} - \mathbf{q}; my + q_z + \frac{m}{M} q_z, l + \mathbf{q} \right] \\ \times \frac{-2}{[(y - Y)q_z + \mathbf{V} \cdot \mathbf{q} + \vec{q}^2 / 2m_R]_P} \frac{e^2}{\vec{q}^2}. \quad (53)$$

We see that we have obtained almost exactly the negative of the expression (51) for the first-order spectator contribution to the cross section. That is, the integrated contribution must be almost exactly zero. The only difference between the two expressions (51) and (53) occurs in the longitudinal-momentum arguments of the wave functions. If these functions did not depend on longitudinal momentum, then the spectator correction to the inclusive cross section (i.e., integrated over spectator momenta) would vanish. This is easy to understand on a heuristic basis. If the wave functions did not depend on the longitudinal momenta of the partons, then the longitudinal position of the two colliding partons would be exactly determined. Thus, the time of formation of the heavy quark would be exactly determined and the effects of the interaction with the light quark would cancel exactly. This case may be contrasted with the case in which the heavy-quark formation time is somewhat uncertain. Then one cancels an evolution operator $U(\infty, t)$

This change of variables has two virtues. First, the transverse-momentum arguments of the two Ψ_B wave functions in Eq. (51) are mapped into each other:

$$\mathbf{P} = \mathbf{P}' - \mathbf{q}', \quad \mathbf{P} - \mathbf{q} = \mathbf{P}'$$

and

$$l = l' + \mathbf{q}', \quad l + \mathbf{q} = l'.$$

Second, the sign of the energy denominator is reversed:

$$\left[(y - Y)q_z + \left[\frac{l}{m} - \frac{\mathbf{P}}{M} \right] \cdot \mathbf{q} + \frac{\vec{q}^2}{2m_R} \right] \\ = - \left[(y' - Y)q'_z + \left[\frac{l'}{m} - \frac{\mathbf{P}'}{M} \right] \cdot \mathbf{q}' + \frac{\vec{q}'^2}{2m_R} \right].$$

Since we integrate over l , \mathbf{q} , and \mathbf{P} , we can drop the primes:

with an evolution operator $U(\infty, t')^\dagger$ for the conjugate state, where the times t and t' are somewhat uncertain. An operator $U(t', t)$ is left over.

We also see that the shifts in the longitudinal-momentum arguments of the Ψ 's are of order m/M , which will evidently lead to a suppression of the coalescence contribution to the cross section by a factor m/M compared to the Born term. The m/M factors are easy to understand. The natural time scale for the spectator interactions is $1/m$. The natural longitudinal size of a hadron is also $1/m$, but the fast quarks in the incoming hadrons are forced into Lorentz-contracted disks of longitudinal size $(1/m) \times (m/M)$. The collision time of the fast quarks is thereby determined to within a time $1/M$. Thus, the Lorentz-contraction factor m/M (the factor appearing in the arguments of the wave functions) leads to a suppression of the contribution by a factor m/M .

When we form the inclusive cross section we integrate over some regions where the Coulomb approximation in

our model is not valid, since the spectator and the heavy quark do not have small relative velocity. Thus, we keep the essential fact of unitarity in the model cross section, but lose the proper properties of one-photon exchange for particles with relativistic relative velocities. We thus expect corrections from the exchange of transversely polarized photons or gluons, although such effects do not lead to low-relative-velocity distortions. We hope to improve the model in a future publication.

We have seen from the above analysis that there is a large enhancement to the Born cross section when $v \ll 1$, but that this enhancement is nearly canceled in the integrated cross section (assuming $M \gg m$). We conclude that there must be a depletion of the cross section in the region of moderate values of v . It is easy to see qualitatively how this comes about. The sign of the first-order cross section in Eq. (38) is determined by the sign of the energy denominator

$$\vec{V} \cdot \vec{q} + \vec{q}^2 / 2m_R = \frac{1}{2m_R} [(m_R \vec{V} + \vec{q})^2 - (m_R \vec{V})^2]. \quad (54)$$

$$\left. \left(\frac{d\sigma}{dY} \right) \right|_{\text{1st order}} = \frac{\pi G^2}{M^2 s} \int d\mathbf{P} dl m dy \frac{d\vec{q}}{(2\pi)^3} \frac{m}{M} \frac{q_z}{m} \frac{\partial}{\partial \lambda} [\Psi_B(x_B^0(1-Y+\lambda))^2 \Psi_A(x_A^0(1+Y-\lambda), \mathbf{P}; m(y-\lambda), l) \\ \times \Psi_A(x_A^0(1+Y-\lambda), \mathbf{P}-\mathbf{q}; m(y-\lambda)+q_z, l+\mathbf{q})]_{\lambda=0} \\ \times \frac{1}{[(y-Y)q_z + \mathbf{V} \cdot \mathbf{q} + \vec{q}^2 / 2m]_p} \frac{e^2}{\vec{q}^2}. \quad (55)$$

From this form, it is apparent that λ inside the square brackets of (55) corresponds to a simultaneous shift in the rapidities of the heavy quark and spectator quark within the wave-function arguments.

C. Further developments of the model

We have seen that the effects of interactions of the heavy quark with light spectator quarks are suppressed by a factor m/M if we integrate over the heavy-quark transverse momentum and do not observe the spectator quarks. We now seek to further refine our understanding of the nature of the leading term that remains after the cancellation. To do so, it will be helpful to consider an explicit model for the wave functions that appear in Eq. (55).

We begin by replacing the squared wave function for hadron B by the parton distribution function:

$$\Psi_B(x_B)^2 \rightarrow f_B(x_B). \quad (56)$$

$$\left. \left(\frac{d\sigma}{dY} \right) \right|_{\text{1st order}} = \alpha \frac{m}{M} \left. \left(\frac{d\sigma}{dY} \right) \right|_{\text{Born}} \int dy d\tau I(y-Y, \tau) \\ \times \left[\rho^{1/2}(y) \rho^{1/2}(y+\tau) \left[-\frac{\partial}{\partial Y} \right] \ln [f_B(x_B^0 e^{-Y}) f_A(x_A^0 e^Y)] - \frac{\partial}{\partial y} [\rho^{1/2}(y) \rho^{1/2}(y+\tau)] \right], \quad (59)$$

where

When $V \ll 1$, there are contributions to the \vec{q} integral in Eq. (38) from regions of both positive and negative values of the energy denominator. We have seen that the net result is positive. When V is larger, the dependence of the wave function on \vec{q} cannot be neglected. The wave function favors values of \vec{q} near $-\vec{l} \approx -m_R \vec{V}$. In this region the energy denominator is negative. Thus, a negative result is obtained.

We can exhibit the sensitivity of the cancellation to wave-function variation more precisely: we extract the leading noncanceling piece of the coalescence correction by taking the average of the expressions (51) and (53), writing the difference of wave functions with slightly different arguments as a derivative. We see that the leading contribution is of order m/M . After extracting this leading contribution, we neglect all of the small terms in the arguments of the wave functions. We also neglect the distinction between m_R and m . The result is

We replace the wave functions for hadron A by factorized distributions representing (1) Gaussian transverse-momentum dependence, (2) x_A dependence for the active quark as given by a standard parton distribution function, and (3) y dependence for the spectator quark given by a probability $\rho(y)dy$ with the function $\rho(y)$ still to be modeled. Thus, we write

$$\Psi_A(x_A, \mathbf{k}, m, y, l)^2 m dy = f_A(x_A) \rho(y) dy \\ \times \frac{1}{\pi^2 m^4} e^{-(\mathbf{k}^2 + l^2)/m^2}. \quad (57)$$

We also adopt the definition

$$\tau = q_z / m. \quad (58)$$

Finally we shall use the appropriate relativistic generalization of the Ψ and f arguments given by the replacement $(1 \pm Y) \rightarrow e^{\pm Y}$. With this replacement we need no longer work in a frame where Y is small.

Given these substitutions, Eq. (55) becomes

$$I(y-Y, \tau) = \frac{1}{2\pi^4 m^6} \int d\mathbf{P} d\mathbf{l} d\mathbf{q} \exp\{-[\mathbf{P}^2 + (\mathbf{P}-\mathbf{q})^2 + l^2 + (l+\mathbf{q})^2]/2m^2\} \\ \times \frac{\tau}{[(y-Y)\tau + \mathbf{V}\cdot\mathbf{q}/m + \tau^2/2 + \mathbf{q}^2/2m^2]_P} \frac{1}{\mathbf{q}^2/m^2 + \tau^2}. \quad (60)$$

Here we may work in the $m/M \rightarrow 0$ limit for \mathbf{V} and thus take $\mathbf{V} = l/m$.

The above form for I may be reduced to

$$I(y-Y, \tau) = \frac{\text{sgn}(\gamma)}{2\pi} \int_0^\infty d\alpha \int_0^\infty \frac{d\beta}{1+\beta} e^{-(\alpha+\tau^2\beta/2)} \frac{1}{(\gamma^2-\alpha\beta)^{1/2}} \Theta(\gamma^2-\alpha\beta), \quad (61)$$

where $\gamma = (y-Y) + \tau/2$.

The magnitude and sign of the first-order correction, Eq. (59), to the inclusive cross section $d\sigma/dY$ are somewhat model dependent. However, a few general conclusions are possible. We focus on the case where the interaction of the heavy quarks with the spectators is attractive. We also assume that the spectator color distribution $\rho(y)$ tends to be concentrated over a limited range of y , $y \approx y_0$. In this case τ will tend to be small in the integral of Eq. (59). We consider three configurations and work in the overall center-of-mass frame, where $E_A = E_B$ and $x_A^0 = x_B^0 = M/\sqrt{s}$.

(1) Very fast heavy quarks with large Y such that $x_A = x_A^0 e^Y \rightarrow 1$. In this case momentum conservation requires that the spectators are concentrated about a small value of y_0 . Since $y-Y < 0$, $I < 0$. For the typical behavior $f(z) \sim (1-z)^p/z$, the logarithmic derivative term in Eq. (59) takes the form

$$-\frac{\partial}{\partial Y} \ln \left[\frac{(1-x_A^0 e^Y)^p (1-x_B^0 e^{-Y})^p}{x_A^0 x_B^0} \right] = \left[\frac{p x_A}{1-x_A} - \frac{p x_B}{1-x_B} \right].$$

The first term in the large brackets of Eq. (59) is thus positive and becomes large since x_A is near 1. The derivative of the second term in brackets with respect to y will be negative for $y < y_0$ and positive for $y > y_0$. Since I is smoothly behaved near $y \sim y_0$, these two regions tend to cancel and this term will be small. Overall we see that the coefficient of m/M is negative and that it can become large in the $x_A \rightarrow 1$ limit of large Y .

(2) Similar rapidities, $y \sim y_0 \sim Y$, for the heavy quark and spectator. This corresponds to momenta for the heavy quark and spectator system in the ratio M/m , i.e., the heavy quark still has substantial Feynman x_F . Depending upon the exact kinetic configuration the structure-function argument x_A may or may not be near an end point; the logarithmic derivative term in the brackets of Eq. (59) will be positive and could be significant in size. However, $I(y-Y, \tau)$ changes sign as we integrate y about $y_0 \sim Y$, and this term will tend to yield a small contribution of uncertain sign. The second term depends upon the correlation between the sign of $I(y-Y, \tau)$ and the y derivative of the ρ 's. For $y < y_0 \sim Y$, I is negative and the ρ derivative term is negative, while for $y > y_0 \sim Y$, I is positive and the ρ derivative term is also positive. Thus the regions combine to yield a possibly sizable (depending upon how peaked ρ is) positive correction.

(3) A slow moving heavy quark with $0 < Y \ll Y_{\max} = \ln(1/x_A^0)$. The main concentration of ρ will correspond to a moderate value of y_0 . Typically

$y-Y > 0$ and I is positive. The f derivative term in Eq. (59) will be positive and not particularly large. As in case 1 the ρ -derivative term changes sign in a region where I varies smoothly, yielding a small contribution. Overall we can obtain a small positive correction.

In all the above regions contributions from spectators contained in incoming hadron B must be included, and serve to symmetrize the correction with respect to the beam and target directions when $A \equiv B$.

To obtain more definitive results would require the development of a detailed picture of the color correlations between the produced heavy quark Q and the spectator system that is singled out in the formula, Eq. (59). A sum over all such spectator systems is required. To the extent that these nonperturbative corrections can eventually be measured, we shall be able to learn more about such color correlations. However, the above analysis indicates that the heavy-quark inclusive cross section will be increased by terms of order m/M for all but very large rapidities Y .

IV. ANOMALOUS FEATURES OF CHARM HADROPRODUCTION

We now turn to an experimental review of those features of charm and bottom hadroproduction that may have a direct connection to the nonperturbative effects discussed in the preceding sections, or are closely related thereto. We first ask whether or not the existing data for heavy-quark production agree with the leading-order QCD predictions. Recent measurements of the total cross section for b jets with $p_T > 5$ GeV and $|y| < 2$, reported by the UA1 Collaboration²⁹ agree well with the lowest-order QCD predictions.³⁰ The theory should be regarded as having, perhaps, a factor of 2 uncertainty due to lack of knowledge of the precise gluon distribution functions and higher-order corrections. It remains to be seen whether or not lowest-order theory will also yield an approximate agreement with experiment for $p_T < 5$ GeV, where the type of corrections we consider here are the largest.

Whether or not the data for charm hadroproduction agree with the leading-order QCD predictions is problematic. For example, the leading fusion contributions predict cross sections which are essentially additive in the nucleon number of a nuclear target. The Fermilab measurements of Ref. 14, however, show an A dependence characteristic of shadowing and diffraction.

An important question for our work is whether or not there is evidence for a *leading-particle effect*; i.e., a correlation of the produced charmed hadron with the hadron beam quantum numbers. This effect is not predicted by

the leading-order QCD predictions.

The $pp \rightarrow \Lambda^c X$ data³¹ from the CERN ISR gave the first indications that charm production may be much flatter in longitudinal momentum than expected from the very central gluon-fusion subprocesses. This appears to be confirmed by Serpukhov data (see Ref. 32) for 40-GeV neutron-carbon collisions: $dN/dx_F (nN \rightarrow \Lambda_c X) \sim (1-x_F)^{1.5 \pm 0.5}$ for $x_F \geq 0.5$. However, recent data from the Lexan Bubble Chamber-European Hybrid Spectrometer (LEBC-EHS) experiment¹² at the CERN SPS for incident 400-GeV/c protons do not show a clear signal for Λ^c production at large x_F . The LEBC experiment has also taken data at Fermilab with a 800-GeV/c proton beam.¹³ Neither LEBC experiment reports a leading-particle effect for D production by protons, and the energy and normalization of the $pp \rightarrow DX$ cross section appears consistent with the simplest QCD estimates. The moderate growth in the magnitude of the D production cross section¹³ with energy also is difficult to reconcile with the ISR results.

Experiments do appear to agree on evidence for a leading particle correlation for charmed hadrons produced by mesons. Recent data for high-energy pion and kaon beams measured by the Amsterdam-Bristol-CERN-Cracow-Munich-Rutherford¹¹ (ACCMOR) and LEBC-EHS (Ref. 12) Collaborations at the SPS show sizable contributions at large x_F , although the statistics are not large. A sample curve from Ref. 12 is given in Fig. 5.

Another intriguing anomaly in charm hadroproduction is seen in the WA-42 experiment¹⁵ at the SPS, which reports copious production of the $A^+(csu)$ (Ξ_c^+) charmed-strange baryon in 135-GeV Σ^- collisions on a beryllium target. Evidence for production of the A^+ in neutron-nucleus collisions has also been reported by the E-400 experiment at Fermilab.¹⁶ In this latter experiment, the cross section appears to be fairly flat over the measured range of $0 < x_F < 0.6$. In the WA-42 experiment the A^+ is observed in the $\Lambda K^- \pi^+ \pi^+$ channel with a hard distribution $(1-x_F)^{1.7 \pm 0.7}$ for $x_F > 0.6$. (A schematic representation of this reaction, to which we shall refer later, is given in Fig. 6.) The corresponding

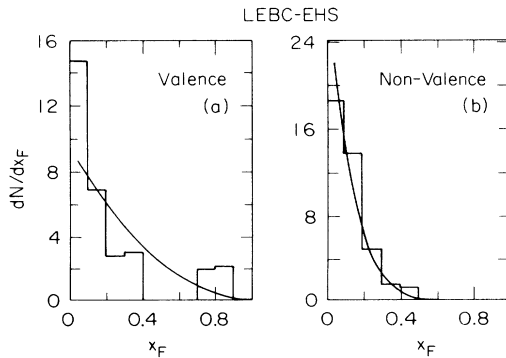


FIG. 5. The x_F distribution for $\pi^- p \rightarrow DX$ at 360 GeV/c measured in the LEBC-EHS experiment (Ref. 12): (a) D mesons containing valence quarks of the pion; (b) nonvalence D mesons. The curves represent fits $(1-x_F)^n$ with $n = 1.8$ and $n = 7.9$, respectively.

cross section times branching ratio (taking the above form for all x_F), for forward x_F is $4.7 \mu\text{b}/\text{nucleon}$, assuming A^1 dependence. If the branching ratio for the measured channel is 3–5%, this implies a total cross section in the 100–150- μb range. Even larger cross sections might be expected for the production of charmed-strange (csd) baryons which carry two valence quarks of the $\Sigma^-(sdd)$. Certainly the experimental results suggest the possibility of systematically enhanced production of heavy-quark states by hyperon and kaon beams.

We now turn to a consideration of the extent to which the above anomalies can be attributed to the prebinding/coalescence enhancements discussed in detail in Sec. III, or to other closely related nonperturbative effects.

V. BREAKDOWN OF FACTORIZATION AND FINAL-STATE-INTERACTION EFFECTS

Let us review from an intuitive viewpoint the impact of the calculations presented in Secs. II and III. We first focus on the process $\gamma \rightarrow \mu^+ \mu^-$ in the presence of the Coulomb field of a nucleus. In Sec. II we found that this QED process fitted into the usual factorization formalism, provided the muons could be considered as having relativistic velocities in the rest frame of the nucleus. Indeed, the eikonal techniques we employed allowed us to obtain a direct understanding of the Born cross section in terms of a hard-scattering process convoluted with the photon distribution function arising from the nucleus. However, we also know (and could demonstrate using techniques such as those presented in Sec. III) that for small velocities of one of the muons relative to the nucleus, the Born cross section is completely unreliable. The cross section is strongly distorted for relative velocities v^+ and v^- of the μ^+ or μ^- with respect to the nucleus $v_{\pm} \ll Z\alpha$ by multiple soft Coulomb interactions.^{6,28}

$$d\sigma(\gamma Z \rightarrow \bar{l}lX) = d\sigma_0 \frac{\xi_+ \xi_-}{(e^{\xi_+} - 1)(1 - e^{-\xi_-})}. \quad (62)$$

Here $d\sigma_0$ is the Bethe-Heitler cross section computed in Born approximation, and $\xi_+ = 2\pi Z\alpha/v^+$, ξ_-

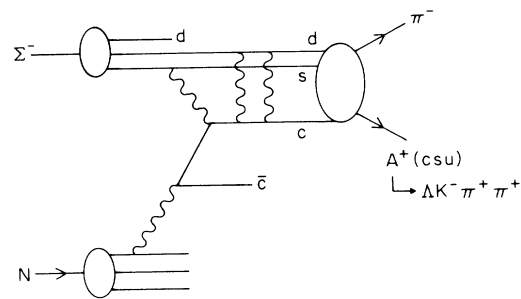


FIG. 6. Schematic representation of A^+ production by hyperon beams. The multigluon exchange can represent either intrinsic-heavy- $c\bar{c}$ contributions to the Σ^- wave function (an initial-state effect) or prebinding distortion from final-state interactions.

$=2\pi Z\alpha/v^-$. These results are strictly valid for $\zeta_+ \ll 1$, but ζ_- can be unrestricted. The effect of the correction factor is to distort the cross section toward small negative-lepton velocity (relative to the target rest frame). As $v^- \rightarrow 0$, the enhancement is so strong that even the threshold phase-space suppression factor in σ_0 is canceled. Conversely, the cross section is exponentially damped when the positive lepton has low velocity.

An analogous effect evidently would also occur in QCD for a heavy colored target. We can estimate³ this QCD prebinding effect by replacing $\pi Z\alpha \rightarrow \frac{4}{3}\pi\alpha_s(Q^2)$ in the QED distortion factor, Eq. (62). (We take Q^2 to be the relative momentum of the c quark with the spectator system, and we limit $|\alpha_s| \leq 4$.) Clearly this gives only a very rough estimate of physics controlled by QCD nonperturbative effects. The behavior predicted by this model indicates significant increases in the magnitude of the heavy-quark production cross sections and significant skewing of the heavy-particle momentum distribution towards large x_F . (See Fig. 7.)

This is not exactly the same as the configuration of interest in establishing a connection with the anomalies found in charm production. There the target is a color-singlet composite of constituents that are relatively light compared to the charm mass scale. In Sec. III we analyzed the QED analogue of the production of a single heavy colored object Q in the presence of such a target. We saw, as expected, that the inclusive cross section for the production of Q exhibited factorization in leading order in M_Q . However, we found corrections to the standard factorized formula for the inclusive cross section of relative order μ/M_Q ; these corrections may be large for charm production. In addition, we examined the case in which spectator particle momenta are measured. In this case, an attractive spectator-heavy-quark interaction can dramatically enhance the cross section in the region in which the light spectator q is moving slowly relative to Q . We also saw that this low-relative-velocity

enhancement must be compensated by depleting the cross section in regions where the q and Q have large relative velocity.

We can now relate these findings to the experimental situations described in the previous section, which appear to exhibit anomalies relative to the perturbative predictions based on factorization. First imagine producing a heavy quark Q at a given rapidity Y , and consider the cross section as a function of the spectator quark q rapidity y . When $y \sim Y$ the cross section will be greatly enhanced, according to the QED analogue results in Sec. III, if the q and Q are in attractive channel. This situation corresponds physically to q and Q being part of the same bound state. Thus, we predict that charmed bound states formed from a charm quark of given Y and a spectator fragment (with $y \sim Y$) will be substantially enhanced over estimates based on perturbative charm production followed by cross-section-conserving "recombination"³³ of the charm quark with spectator quarks. However, to avoid inconsistency with the predicted higher-twist nature of the inclusively integrated spectrum, there must be a compensating depletion of the cross section in other configurations, such as where y is sufficiently different from Y that the charm-quark and spectator-quark fragment independently into the observed final-state hadrons. The net effect will be a redistribution of the inclusive charm cross section in favor of those charmed hadrons whose location in rapidity and whose quark content can both be clearly identified as requiring spectator-quark content. This is what is observed, i.e., enhanced production of charm in the forward low- p_T region, especially when contained in hadrons, such as the Λ_c , that are clearly most likely to arise as a combination of fast spectators with a charm quark of similar rapidity.

As discussed in Sec. III, the inclusively integrated spectrum depends upon the detailed distribution of color charge in the spectator system. Unless the heavy-quark color is primarily balanced by that of a spectator of very similar rapidity, the enhancement of recombination bound states is likely to be rather closely compensated by depletion in the spectrum of hadrons containing the heavy quark that are formed by independent fragmentation. In the case of charm, the higher-twist restoring depletion would occur in the spectrum of hadrons that are most likely the result of independent fragmentation of the produced charm quark. Experimental determination of the inclusive heavy-quark spectrum is not trivial. It requires summing over the inclusive cross sections for all hadrons containing the heavy quark.

As we have emphasized, unlike final-state interaction corrections to hard-scattering processes, the corrections discussed in this paper to semi-inclusive production of states containing a heavy quark and spectator in an attractive channel, coherently enhance the production process and are not limited by unitarity to be of order one. If there are not strange quarks in the incident hadron, then the distortion and enhancements in cross sections for spectator-containing hadrons are likely to be magnified, since a strange quark tends to be more nonrelativistic than u or d quarks in a hadron and thus more effective

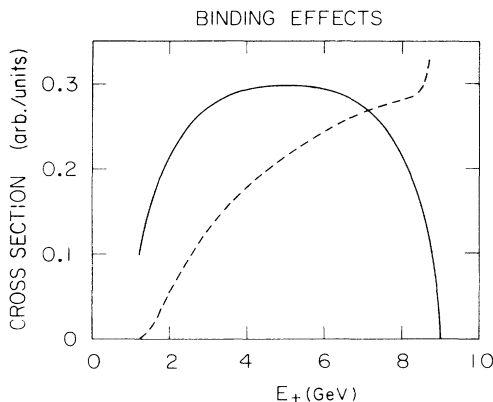


FIG. 7. The Bethe-Heitler cross section $\gamma Z \rightarrow l^+ l^- Z$ in Born approximation (solid curve) as a function of the positive-lepton energy. The dotted curve shows the modified spectrum due to multiple scattering $Z\alpha \rightarrow \frac{4}{3}\alpha_s(Q^2)$. We have used $\alpha_s(Q^2) = 4\pi/[\beta_0 \ln(1+Q^2/\Lambda^2)]$, $|\alpha_s| < 4$, where $\Lambda = 200$ MeV and Q^2 is the four-momentum squared to the target. The incident energy is 10 GeV.

in “capturing” the heavy quarks that tend to be produced moving slowly in the laboratory frame. This could explain the relatively copious production of the $A^+(csu)$ in the Σ^- fragmentation region, and suggests an important role of hyperon and strange meson beams for charm and heavy-particle-production experiments.

Finally, we would like to point out that there are several tests of the basic Sommerfeld correction underlying coalescence that can be performed in the near future. In the attractive channel $e^+e^- \rightarrow Q\bar{Q}$, near threshold, enhancement in the form of resonances occur, and these resonances are more or less dual to the enhanced perturbative cross section. A similar result is expected for the reaction $e^+e^- \rightarrow \gamma Q\bar{Q}$ in the region where the final state γ has large p_T and the $Q\bar{Q}$ system has low mass. In contrast, the reaction $e^+e^- \rightarrow gQ\bar{Q}$ corresponds to the $Q\bar{Q}$ being a repulsive color channel, and, in the region where the g has high p_T and the $Q\bar{Q}$ invariant mass is low, a *diminished* cross section (with respect to the perturbative prediction) should be observed. One can compute in perturbation theory the magnitude of the repulsive color factor in this latter situation compared to that for the former attractive case. One obtains a $\frac{4}{3}$ in the color-singlet attractive channel and $-\frac{1}{6}$ in the color-octet repulsive channel, where the relative sign indicates that the first is repulsive and the second attractive. Of course, the attractive channel will actually contain bound states below and resonances above the zero velocity threshold. A dual average over the region near threshold in the attractive channel must be compared to the average over the appropriate small-velocity region of the repulsive channel in order to determine the enhancement and diminishment of the two channels relative to the Born graph expectations. This prediction may already be testable using available data.

Similarly in the reaction $gg \rightarrow gQ\bar{Q}$, studied perturbatively in Refs. 7 and 8, a high- p_T g trigger, coupled with low invariant mass for the $Q\bar{Q}$ system corresponds to a repulsive $Q\bar{Q}$ channel (on average) and overall suppression with respect to the lowest-order perturbative prediction is predicted. Relative to the above color group factors this channel also has weight $-\frac{1}{6}$. In repulsive channels the Q and \bar{Q} would presumably end up in a $Q\bar{Q}$ bound state rather infrequently, preferring to fragment independently into hadrons containing Q or \bar{Q} , respectively. Summing over all such production modes would be required before comparison with the perturbative prediction.

VI. INTRINSIC HEAVY QUARKS

We turn now to a brief consideration of other nonperturbative and anomalous effects that could also play a role in explaining the experimental data reviewed in Sec. IV. The intrinsic heavy-quark concept, discussed in this section, is closely allied to the ideas of coalescence: the latter is a nonperturbative final-state reinteraction effect, while the former arises from initial-state interactions. Both are predicted to be higher-twist contributions at the fully integrated inclusive cross-section level, but yield enhancements in special regions of phase space. Since

the momentum of a charmed hadron tends to follow the momentum of the produced charmed quarks (the Bjorken-Suzuki effect³⁴), the longitudinal-momentum dependence of the charm hadroproduction data suggest that the charm quarks themselves have large momentum fraction in the nucleon. Such a possibility can be checked by measurements of deep-inelastic scattering of leptons on the charm constituents of the nucleon. The available high- Q^2 data from the EMC (Ref. 17), as extracted from $\mu N \rightarrow \mu\mu X$ data, seem to indicate an anomalously large $c(x, Q^2)$ distribution at large Q^2 and $x_{\text{Bj}} \sim 0.4$ compared to that expected for the proton-gluon fusion diagrams or, equivalently, from QCD evolution.³⁵ Although the data have low statistics and thus could be misleading, it suggests the existence of mechanisms for charm production other than the standard photon-gluon fusion subprocess.

Dimension-six contributions to the effective Lagrangian imply the existence of Fock states in the nucleon containing an extra $Q\bar{Q}$ pair.²² (See Fig. 8.) Eventually nonperturbative methods such as lattice gauge theory or discretized light-cone quantization³⁶ should be able to determine the heavy-particle content of meson and baryon wave functions. At this time we can deduce^{22,37} the following semiquantitative properties for intrinsic states such as $|uudQ\bar{Q}\rangle$. (1) The probability of such states in the nucleon is nonzero and scales as M_Q^{-2} . (2) The maximal wave-function configurations tend to have minimum off-shell energy, corresponding to constituents of equal velocity or rapidity, i.e.,

$$x_i \equiv \frac{(k^0 + k^z)_i}{p^0 + p^z} \propto [(k_\perp^2 + m^2)_i]^{1/2}. \quad (63)$$

Thus, intrinsic heavy quarks tend to have the largest momentum fraction in the proton wave function, just opposite to the usual configuration expected for sea quarks. (3) The transverse momenta of the heavy quarks are roughly equal and opposite and of order M_Q , whereas the light quarks tend to have soft momenta set by the hadron wave function. (4) The effects are strongly dependent on the features of the valence wave function; the intrinsic heavy-quark probability is thus presumably larger in baryons than in mesons, nonadditive in nucleon number in heavy nuclei, and sensitive to the presence of strange quarks. In deep-inelastic scattering on an intrinsic charm quark the heavy-quark spectator will be found predominantly in the target-fragmentation region.

The intrinsic charm structure function will not become fully observable unless the available energy is well above threshold: $W = (q + p)^2 \gg W_{\text{th}}^2 = 4M_Q^2$. The correct rescaling variable for deep-inelastic muon scattering is roughly $x = x_{\text{Bj}} + W_{\text{th}}^2/W^2$, not

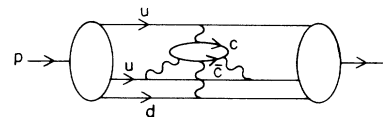


FIG. 8. Representation of an intrinsic heavy-quark Fock state in the proton.

$x = x_{Bj} + M_Q^2/Q^2$ which is appropriate to charge-current single heavy-quark excitation.

The presence of a hard-valence-like charm distribution in the nucleon can, at least qualitatively, explain some of the anomalous features of the charm hadroproduction data discussed above. The fact that the c and \bar{c} as well as D and \bar{D} distributions are harder than the corresponding strange-particle distributions can be attributed to the fact that the skewing of quark distributions to large x only really becomes effective for quarks heavier than the average momentum scale in the nucleon. One can account for leading-particle effects and the fairly flat Λ_c ISR and Serpukhov cross sections if there is coalescence of the intrinsic charm quarks with the u and d spectator quarks of the nucleons. We note that recombination itself cannot explain the comparable distributions observed in the LEBC experiment for proton production of D and \bar{D} , unless it is the heavy quarks that carry most of the momentum. Since the intrinsic contribution is associated with higher-twist operators, it is suppressed by a factor of $1/M_Q^2$ relative to the fusion contributions, and is thus unlikely to be very important for b - or t -quark hadroproduction.

The presence of intrinsic charm quarks in the nucleons also has implications for other hard-scattering processes involving incident charmed quarks. In general, the charm quark in the nucleon will reflect both extrinsic and intrinsic ($1/M_c^2$) contributions. Using QCD factorization this implies significant intrinsic charm contributions to hard-scattering processes such as $c + g \rightarrow c + X$ at $p_T^2 \gg 4M_c^2$, with the intrinsic contribution dominating the large- x domain. The characteristic signal for such contributions is a \bar{c} spectator jet in the beam-fragmentation region. Similarly, heavier quarks and supersymmetric particles of mass \bar{m} contribute to intrinsic Fock states in the nucleon at order $1/\bar{m}^2$. The intrinsic $\bar{q}(x)$ or $\bar{g}(x)$ distribution is again predicted to be largest at large x . Hard-scattering processes such as $\bar{q} + \bar{q} \rightarrow \bar{\gamma} + \gamma$ can produce purely electromagnetic mono-jet events. Note that the associated intrinsic supersymmetric partner appears in the beam-fragmentation region.

VII. DIFFRACTIVE HARD PROCESSES

We review this type of process as another example of a situation in which the results for heavy-quark production cannot be obtained perturbatively, and, thus, experiments involving heavy-quark production could shed light on the nature of nonperturbative QCD. The situation of interest is that where production of the heavy-quark system occurs diffractively in the hadron collision, that is, without excitation of the target. Two pictures have been given for this processes.

(1) Diffractive excitation.²⁴ When a beam hadron fluctuates into a Fock state such that all of its constituents are at small relative impact parameter, it interacts minimally because of its small color-dipole moment. Since the normal states interact strongly, the small impact valence Fock state materialize as $q\bar{q}$ or qqq jets. In the case of intrinsic heavy-quark Fock states $qqqQ\bar{Q}$ with

small transverse size, the incoming nucleon can be diffractively excited into a forward-produced system containing a heavy-quark pair. An analysis of such processes based on the Good and Walker two-component formalism is given in Ref. 24.

(2) The Pomeron as a gluon source.^{38,18} If one treats the Pomeron as a composite system with gluon constituents, then the gluon-gluon fusion process leads to diffractively produced heavy-quark systems. The analysis of such processes is given in Ref. 38.

Both pictures of diffractive production lead to similar final states and cross-section estimates. In particular, the total production rate has a predicted nominal nuclear-number dependence $\sigma \sim A^{2/3}$. However, the x_F distribution of the heavy-quark system tends to be harder and the mass of the diffractive system smaller in the intrinsic-charm picture.³⁹

Experimental investigations of such processes could significantly further our understanding of nonperturbative QCD. Note that for sufficiently heavy quarks, the perturbative description based on Eq. (1) should become valid, and diffractive excitation can be viewed as gluon fusion involving a gluon from the target carrying a very small longitudinal-momentum fraction. (See Ref. 1). Thus, in the heavy-quark-mass limit, the two pictures of diffractive processes become two different views of the same physics.

VIII. SUMMARY

There is little doubt that the standard perturbative QCD predictions are accurate for very massive heavy-quark production. Indeed, the two calculations in this paper confirm that corrections to the standard factorization formalism are suppressed by powers of the heavy-quark mass. Nevertheless, there are interesting and important corrections at low transverse momentum in the beam and target-fragmentation regions when the quark mass is not too large. These are the kinematic regions where intrinsic contributions may appear and coherent effects can occur as the produced quark and spectator fragments coalesce. As reviewed here, the data appear to have anomalies in these regions. It is clearly very important to verify these effects, particularly leading-particle effects, enhancements due to hyperon beams, the A dependence, the importance of diffractive production, and leading-particle effects. From the theoretical perspective, the charm-production data provide a window to the interface of perturbative and nonperturbative dynamics.

ACKNOWLEDGMENTS

We would like to thank J. Bjorken, J. C. Collins, A. Mueller, D. Potter, and P. Zerwas for helpful conversations. This work was supported by the Department of Energy, Contract No. DE-AC03-76SF00515.

APPENDIX

We wish to evaluate the integral (14) for the muon pair production cross section:

$$d\sigma/dz_C dz_D = \frac{1}{2} M^2 e^2 z_C z_D \delta(1-z_C-z_D) (2\pi)^{-3} \\ \times \int d^2\mathbf{x}_C \int d^2\mathbf{x}_D K_0(M|\mathbf{x}_C-\mathbf{x}_D|)^2 [2-(\mathbf{x}_C^2/\mathbf{x}_D^2)^{+iZ\alpha} - (\mathbf{x}_C^2/\mathbf{x}_D^2)^{-iZ\alpha}]. \quad (\text{A1})$$

We begin by writing this integral in the form

$$d\sigma/dz_C dz_D = \frac{1}{2} M^2 e^2 z_C z_D \delta(1-z_C-z_D) (2\pi)^{-3} \int d^2\mathbf{r} K_0(M|\mathbf{r}|)^2 r^2 I(0), \quad (\text{A2})$$

where the integral $I(\epsilon)$ is defined by

$$I(\epsilon) = r^{-2+2\epsilon} \int d^2\mathbf{x}_C \int d^2\mathbf{x}_D |\mathbf{x}_C|^{-\epsilon} |\mathbf{x}_D|^{-\epsilon} \delta(\mathbf{x}_C-\mathbf{x}_D-\mathbf{r}) [2-(\mathbf{x}_C^2/\mathbf{x}_D^2)^{+iZ\alpha} - (\mathbf{x}_C^2/\mathbf{x}_D^2)^{-iZ\alpha}]. \quad (\text{A3})$$

[$I(0)$ contains the infrared divergence discussed in Sec. II. Here the parameter ϵ , instead of a scattering length, regulates this divergence.] On dimensional grounds, one knows that $I(\epsilon)$ is independent of \mathbf{r} . Thus, the integral of the Bessel function can be performed immediately to give

$$\int d^2\mathbf{r} K_0(M|\mathbf{r}|)^2 r^2 = 2\pi/3M^4. \quad (\text{A4})$$

This leaves the integral $I(\epsilon)$. It can be evaluated by considering the integral

$$J(\epsilon) = \int d^2\mathbf{r} \exp(i\mathbf{q}\cdot\mathbf{r}) r^{2-2\epsilon} I(\epsilon). \quad (\text{A5})$$

On one hand,

$$J(\epsilon) = \pi(\mathbf{q}^2/4)^{-2+\epsilon} [\Gamma(2-\epsilon)/\Gamma(-1+\epsilon)] I(\epsilon). \quad (\text{A6})$$

On the other hand, one can perform the integral for $J(\epsilon)$ as a sum of products of Fourier transforms of a pure power of $|\mathbf{x}|$:

$$J(\epsilon) = \int d^2\mathbf{x}_C \int d^2\mathbf{x}_D \exp(i\mathbf{q}\cdot\mathbf{x}_C - i\mathbf{q}\cdot\mathbf{x}_D) |\mathbf{x}_C|^{-\epsilon} |\mathbf{x}_D|^{-\epsilon} [2-(\mathbf{x}_C^2/\mathbf{x}_D^2)^{+iZ\alpha} - (\mathbf{x}_C^2/\mathbf{x}_D^2)^{-iZ\alpha}] \\ = 2\pi^2 (\mathbf{q}^2/4)^{-2+\epsilon} \left[\frac{\Gamma(1-\frac{1}{2}\epsilon)^2}{\Gamma(\frac{1}{2}\epsilon)^2} - \frac{\Gamma(1-\frac{1}{2}\epsilon+iZ\alpha)\Gamma(1-\frac{1}{2}\epsilon-iZ\alpha)}{\Gamma(\frac{1}{2}\epsilon-iZ\alpha)\Gamma(\frac{1}{2}\epsilon+iZ\alpha)} \right]. \quad (\text{A7})$$

Thus, we can identify

$$I(\epsilon) = 2\pi \left[\frac{\Gamma(-1+\epsilon)\Gamma(1-\frac{1}{2}\epsilon)^2}{\Gamma(2-\epsilon)\Gamma(\frac{1}{2}\epsilon)^2} - \frac{\Gamma(-1+\epsilon)(\frac{1}{2}\epsilon-iZ\alpha)\Gamma(1-\frac{1}{2}\epsilon-iZ\alpha)(\frac{1}{2}\epsilon+iZ\alpha)\Gamma(1-\frac{1}{2}\epsilon+iZ\alpha)}{\Gamma(2-\epsilon)\Gamma(1+\frac{1}{2}\epsilon-iZ\alpha)\Gamma(1+\frac{1}{2}\epsilon+iZ\alpha)} \right]. \quad (\text{A8})$$

We can now expand about $\epsilon=0$, using

$$\Gamma(\frac{1}{2}\epsilon) = (2/\epsilon)(1-\frac{1}{2}\gamma\epsilon + \dots), \\ \Gamma(1-\frac{1}{2}\epsilon) = 1 + \frac{1}{2}\gamma\epsilon, \\ \Gamma(-1+\epsilon) = (1/\epsilon)[1+(1+\gamma)\epsilon + \dots], \\ \Gamma(2-\epsilon) = 1 - (1-\gamma)\epsilon + \dots, \\ \Gamma(X \pm \frac{1}{2}\epsilon) = \Gamma(X)[1 \pm \frac{1}{2}\epsilon\psi(X) + \dots],$$

where $\gamma = 0.577\dots$ is Euler's constant. This gives

$$I(\epsilon) = -2\pi(Z\alpha)^2(1/\epsilon+2) + 2\pi(Z\alpha)^2[\psi(1-iZ\alpha) + \psi(1+iZ\alpha) + 2\gamma] \\ = -2\pi(Z\alpha)^2(1/\epsilon+2) + 4\pi \sum_{n=0}^{\infty} (-1)^n \zeta(2n+3)(Z\alpha)^{2n+4}, \quad (\text{A9})$$

where ζ is the Riemann ζ function.

We can now assemble the result:

$$d\sigma/dz_C dz_D = (e^2/12\pi M^2) z_C z_D \delta(1-z_C-z_D) \{ -(Z\alpha)^2(1/\epsilon+2) + (Z\alpha)^2[\psi(1-iZ\alpha) + \psi(1+iZ\alpha) + 2\gamma] \}. \quad (\text{A10})$$

This is the result reported in Sec. II.

Notice that in Eq. (A1) the dominant contributions come from $|\mathbf{x}_C-\mathbf{x}_D| \sim 1/M$. However, there is an infrared divergence coming from the region $|\mathbf{x}_C| \sim |\mathbf{x}_D| \gg 1/M$. In the calculation, this divergence has been regulated by the factor $(|\mathbf{x}_C| |\mathbf{x}_D|)^{-\epsilon}$. Thus, contributions from this large-impact-parameter region appear as a factor of $1/\epsilon$ in the calculation. Finally, as expected from the argument early in Sec. II, this $1/\epsilon$ appears only in the Born term.

- ¹J. C. Collins, D. E. Soper, and G. Sterman, Nucl. Phys. **B263**, 37 (1986).
- ²G. T. Bodwin, Phys. Rev. D **31**, 2616 (1985); J. C. Collins, D. E. Soper, and G. Sterman, Phys. Lett. **134B**, 263 (1984); C. T. Sachrajda, in *Nuclear Chromodynamics: Quarks and Gluons in Particles and Nuclei*, proceedings, Santa Barbara, California, 1985, edited by S. Brodsky and E. Moniz (World Scientific, Singapore, 1986).
- ³J. F. Gunion and S. J. Brodsky, in *The Sixth Quark*, proceedings of the 12th SLAC Summer Institute on Particle Physics, Stanford, California, edited by P. M. McDonough (SLAC Report No. 281, Stanford, 1985), p. 603; J. F. Gunion, in *Nuclear Chromodynamics: Quarks and Gluons in Particles and Nuclei* (Ref. 2), p. 44; S. J. Brodsky, in *Proceedings of the 23rd International Conference on High Energy Physics*, Berkeley, California, 1986, edited by S. Loken (World Scientific, Singapore, 1987).
- ⁴J. Schwinger, *Particles, Sources, and Fields* (Addison-Wesley, Reading, MA 1973). For other applications and references see S. J. Brodsky, G. Kopp, and P. M. Zerwas, Phys. Rev. Lett. **58**, 443 (1987).
- ⁵H. Bethe and L. Maximon, Phys. Rev. **93**, 768 (1954); H. Davies *et al.*, *ibid.*, **93**, 788 (1954). See also T. Jaroszewicz and J. Wosiek, Acta Phys. Pol. **B8**, 837 (1977); R. Blankenbecler and S. D. Drell, Phys. Rev. D **36**, 2846 (1987).
- ⁶A. Sommerfeld, Ann. Phys. (N.Y.) **11**, 257 (1931).
- ⁷J. F. Gunion and Z. Kunszt, Phys. Lett. B **178**, 296 (1986).
- ⁸R. K. Ellis and J. C. Sexton, Nucl. Phys. **B282**, 642 (1987); R. K. Ellis, in *Strong Interactions and Gauge Theories*, proceedings of the 21st Rencontre de Moriond, Les Arcs, France, 1986, edited by J. Tran Thanh Van (Editions Frontières, Gif-sur-Yvette, France, 1986), p. 339. Analogous QED/QCD asymmetries are discussed in S. J. Brodsky, C. E. Carlson, and R. Suaya, Phys. Rev. D **14**, 2264 (1976).
- ⁹I. Y. Bigi, J. Kuhn, and P. M. Zerwas, Phys. Lett. **157B**, 181 (1986).
- ¹⁰T. K. Gaisser and F. Halzen, in *Progress in Electroweak Interactions*, proceedings of the 21st Rencontre de Moriond, Les Arcs, France, 1986, edited by J. Tran Thanh Van (Editions Frontières, Gif-sur-Yvette, France, 1986), p. 541.
- ¹¹ACCMOR Collaboration, H. Becker *et al.*, work presented at 23rd International Conference on High Energy Physics, Berkeley, California, 1986 (unpublished).
- ¹²LEBC-EHS Collaboration, M. Aguilar-Benitez *et al.*, Z. Phys. C **31**, 491 (1986); Phys. Lett. **135B**, 237 (1984); B. Vonck (unpublished).
- ¹³LEBC-MPS Collaboration, R. Ammar *et al.*, Phys. Lett. B **183**, 110 (1987).
- ¹⁴M. E. Duffy *et al.*, Phys. Rev. Lett. **55**, 1816 (1985); A. Bodek *et al.*, in *Proceedings of the 22nd International Conference on High Energy Physics*, Leipzig, 1984, edited by A. Meyer and E. Wieczorek (Akademie der Wissenschaften der DDR, Zeuthen, East Germany, 1984), Vol. I, p. 157; M. MacDermott and S. Reucroft, Phys. Lett. B **184**, 108 (1987).
- ¹⁵S. F. Biagi *et al.*, Z. Phys. C **28**, 175 (1985).
- ¹⁶The charmed-strange baryon has also been observed in neutron-nucleus collisions at Fermilab. See P. Coteus *et al.*, Phys. Rev. Lett. **59**, 1530 (1987).
- ¹⁷M. Arneodo *et al.*, Report No. CERN-EP/86-88, 1986 (unpublished); J. J. Aubert *et al.*, Phys. Lett. **110B**, 73 (1982).
- ¹⁸E. Berger, J. C. Collins, D. E. Soper, and G. Sterman, Nucl. Phys. **B286**, 704 (1987).
- ¹⁹S. J. Brodsky, G. T. Bodwin, and G. P. Lepage, in *Multiparticle Dynamics, 1982*, proceedings of the XII International Symposium, Volendam, Netherlands, 1982, edited by W. Kittel, W. Metzger, and A. Stergiou (World Scientific, Singapore, 1983), p. 841; in *Proceedings of the Workshop on Drell-Yan Processes*, Batavia, Illinois, 1982 (Fermilab, Batavia, IL, 1983), p. 105.
- ²⁰H. E. Haber, D. E. Soper, and R. M. Barnett, in *Physics Simulations at High Energy*, Madison, Wisconsin, 1986, edited by V. Barger, T. Gottschalk, and F. Halzen (World Scientific, Singapore, 1987).
- ²¹G. T. Bodwin, S. J. Brodsky, and G. P. Lepage, Phys. Rev. Lett. **47**, 1799 (1981).
- ²²S. J. Brodsky, C. Peterson, and N. Sakai, Phys. Rev. D **23**, 2745 (1981); S. J. Brodsky, P. Hoyer, C. Peterson, and N. Sakai, Phys. Lett. **93B**, 451 (1980).
- ²³S. J. Brodsky, J. C. Collins, S. D. Ellis, J. F. Gunion, and A. H. Mueller, in *Proceedings of the Workshop on the Design and Utilization of the SSC, 1984*, edited by R. Donaldson and J. G. Mortin (Fermilab, Batavia, IL, 1985), p. 227.
- ²⁴G. Bertsch, S. J. Brodsky, A. S. Goldhaber, and J. F. Gunion, Phys. Rev. Lett. **47**, 297 (1981).
- ²⁵See also T. Jaroszewicz and J. Wosiek, Acta Phys. Pol. **B8**, 837 (1977).
- ²⁶J. D. Bjorken, J. B. Kogut, and D. E. Soper, Phys. Rev. D **3**, 1382 (1971); H. Cheng, J. K. Walker, and T. T. Wu, *ibid.* **11**, 68 (1975).
- ²⁷J. C. Collins and D. E. Soper, Nucl. Phys. **B194**, 445 (1982); G. Curci, W. Furmanksi, and R. Petronzio, *ibid.* **175**, 27 (1980).
- ²⁸A. I. Akhiezer and V. B. Berestetsky, *Quantum Electrodynamics* (Translation) (Technical Information Service Extension, Washington, D.C., 1953).
- ²⁹T. Markiewicz, in *Proceedings of the 23rd International Conference on High Energy Physics* (Ref. 3).
- ³⁰E. Berger, J. C. Collins, and D. E. Soper, Phys. Rev. D **35**, 2272 (1987).
- ³¹For reviews, see A. Kernan and G. Van Dalen, Phys. Rep. **106**, 6 (1984); S. Reucroft, in *Strong Interactions and Gauge Theories* (Ref. 8); S. J. Brodsky, in *Multiparticle Dynamics, 1985*, proceedings of the 16th International Symposium, Kiryat Anavim, Israel, 1985, edited by J. Grunhaus (Editions Frontières, Gif-sur-Yvette, France, 1985).
- ³²A. N. Aleev *et al.*, Yad. Fiz. **35**, 1175 (1982) [Sov. J. Nucl. Phys. **35**, 687 (1982)].
- ³³R. C. Hwa, in *Proceedings of the II International Symposium on Hadron Structure and Multiparticle Production, Kazimierz, Poland, 1979*, edited by Z. Ajduk (Institute of Theoretical Physics, Warsaw, 1979), p. 9; U. P. Sukhatme, in *Multiparticle Dynamics 1985* (Ref. 31).
- ³⁴J. D. Bjorken, Phys. Rev. D **17**, 171 (1978); M. Suzuki, Phys. Lett. **71B**, 139 (1977).
- ³⁵E. Hoffmann and R. Moore, Z. Phys. C **20**, 71 (1983).
- ³⁶T. Eller, H.-C. Pauli, and S. J. Brodsky, Phys. Rev. D **35**, 1493 (1987), and references therein.
- ³⁷S. J. Brodsky, H. E. Haber, and J. F. Gunion, in *Anti-pp Options for the Supercollider*, Division of Particles and Fields Workshop, Chicago, Illinois, 1984, edited by J. E. Pilcher and A. R. White (SSC-ANL Report No. 84/01/13, Argonne, IL, 1984), p. 100.
- ³⁸G. Ingelman and P. E. Schlein, Phys. Lett. **152B**, 256 (1985); H. Fritzsch and K. H. Streng, *ibid.* **164B**, 391 (1985); K. H. Streng, *ibid.* **166B**, 443 (1986).
- ³⁹We wish to thank D. Potter for discussions on experimental tests of heavy-quark diffractive excitation.